Article

Current Biology

Extracellular ATP facilitates cell extrusion from epithelial layers mediated by cell competition or apoptosis

Graphical abstract

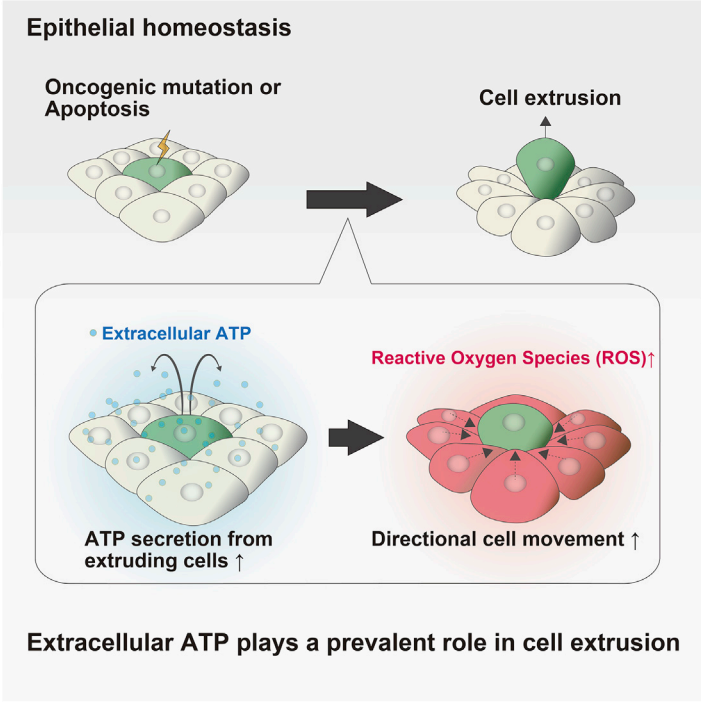

Extracellular ATP plays a prevalent role in cell extrusion

Authors

Yusuke Mori, Naoka Shiratsuchi, Nanami Sato, ..., Yukinari Haraoka, Tohru Ishitani, Yasuyuki Fujita

Correspondence

fujita@monc.med.kyoto-u.ac.jp

In brief

Mori et al. show that during either cell-competition-mediated extrusion or apoptotic extrusion, ATP is secreted from extruding cells, which promotes the ROS level and regulates the polarized movements of surrounding cells toward extruding cells. Thus, extracellular ATP acts as an "extrude me"' signal and plays a prevalent role in cell extrusion.

Highlights

- ROS level is elevated in epithelia around extruding transformed or apoptotic cells
- ATP is extracellularly secreted from extruding cells, which promotes the ROS level
- Extracellular ATP and ROS regulate the polarized movement of the surrounding cells
- Extracellular ATP and ROS promote the extrusion of transformed or apoptotic cells

Mori et al., 2022, Current Biology *32*, 2144–2159
May 23, 2022
https://doi.org/10.1016/j.cub.2022.03.057

CellPress

CellPress

Current Biology

Article

Extracellular ATP facilitates cell extrusion from epithelial layers mediated by cell competition or apoptosis

Yusuke Mori,[1,2] Naoka Shiratsuchi,[1] Nanami Sato,[1,2] Azusa Chaya,[1] Nobuyuki Tanimura,[1,2] Susumu Ishikawa,[2] Mugihiko Kato,[2] Ikumi Kameda,[2] Shunsuke Kon,[2] Yukinari Haraoka,[3] Tohru Ishitani,[3] and Yasuyuki Fujita[1,2,4,*]

[1]Department of Molecular Oncology, Graduate School of Medicine, Kyoto University, Yoshida-Konoe-Cho, Sakyo-Ku, Kyoto-city, Kyoto 606-8501, Japan

[2]Division of Molecular Oncology, Institute for Genetic Medicine, Hokkaido University Graduate School of Chemical Sciences and Engineering, Kita-15 Nishi-7, Kita-Ku, Sapporo 060-0815, Japan

[3]Department of Homeostatic Regulation, Division of Cellular and Molecular Biology, Research Institute for Microbial Diseases, Osaka University, 3-1 Yamadaoka, Suita, Osaka 565-0871, Japan

[4]Lead contact

*Correspondence: fujita@monc.med.kyoto-u.ac.jp

https://doi.org/10.1016/j.cub.2022.03.057

SUMMARY

For the maintenance of epithelial homeostasis, various aberrant or dysfunctional cells are actively eliminated from epithelial layers. This cell extrusion process mainly falls into two modes: cell-competition-mediated extrusion and apoptotic extrusion. However, it is not clearly understood whether and how these processes are governed by common molecular mechanisms. In this study, we demonstrate that the reactive oxygen species (ROS) levels are elevated within a wide range of epithelial layers around extruding transformed or apoptotic cells. The downregulation of ROS suppresses the extrusion process. Furthermore, ATP is extracellularly secreted from extruding cells, which promotes the ROS level and cell extrusion. Moreover, the extracellular ATP and ROS pathways positively regulate the polarized movements of surrounding cells toward extruding cells in both cell-competition-mediated and apoptotic extrusion. Hence, extracellular ATP acts as an "extrude me" signal and plays a prevalent role in cell extrusion, thereby sustaining epithelial homeostasis and preventing pathological conditions or disorders.

INTRODUCTION

To preserve its barrier function and structural integrity, the epithelium possesses several homeostatic mechanisms. Among them, cell extrusion is one of the most crucial processes by which aberrant or dysfunctional cells are actively eliminated from epithelial layers to maintain a healthy, homogenous cellular society.[1–5] There are two major types of cell extrusion: cell-competition-mediated extrusion and apoptotic extrusion; both phenomena are evolutionarily conserved, at least partly, from flies to mammals. Cell competition is a process through which cells with different properties compete with each other for survival and space; aberrant or dysfunctional cells often become loser cells and are eventually eliminated from tissues, whereas the surrounding normal cells become winner cells that proliferate and fill the vacant spaces.[6–15] It has been demonstrated that normal epithelial cells can recognize and actively eliminate the neighboring oncogenically transformed cells via cell competition, implying that normal epithelia have an antitumor activity that does not involve immune cells. This tumor-suppressive phenomenon within epithelia is termed epithelial defense against cancer (EDAC).[16,17] In EDAC, transformed cells are eliminated in either cell-death-independent or cell-death-dependent manner. For instance, in vertebrates, when oncoprotein Ras-, Src-, or ErbB2-transformed cells are surrounded by normal cells, transformed cells are extruded into the apical lumen of the epithelial layer in a cell-death-independent fashion.[18–20] In contrast, tumor suppressor protein Scribble- or Lgl (lethal giant larvae)-deficient cells undergo apoptosis when surrounded by normal epithelial cells and are eventually eliminated from epithelia in *Drosophila* and mammals.[21–24] In addition to these cell-competition-mediated cell extrusions, when apoptosis is induced independently of cell competition (e.g., UV irradiation or caspase activation), the apoptotic cells are extruded from the epithelial layer.[25–28] These different types of cell extrusion are currently regarded as distinct cellular processes, and it remains elusive whether and how common molecular mechanisms are involved in these homeostatic phenomena.

When cells receive physical or chemical insults including hypoxia, injury, inflammation, and apoptosis, ATP is often secreted from stressed cells into the extracellular spaces.[29–33] Extracellular ATP can then act as a signaling molecule that binds to membrane receptors P2X or P2Y, thereby affecting multiple cellular processes such as the production of reactive oxygen species (ROS), leading to the maintenance of tissue homeostasis.[31,33] The excess production of ROS can damage

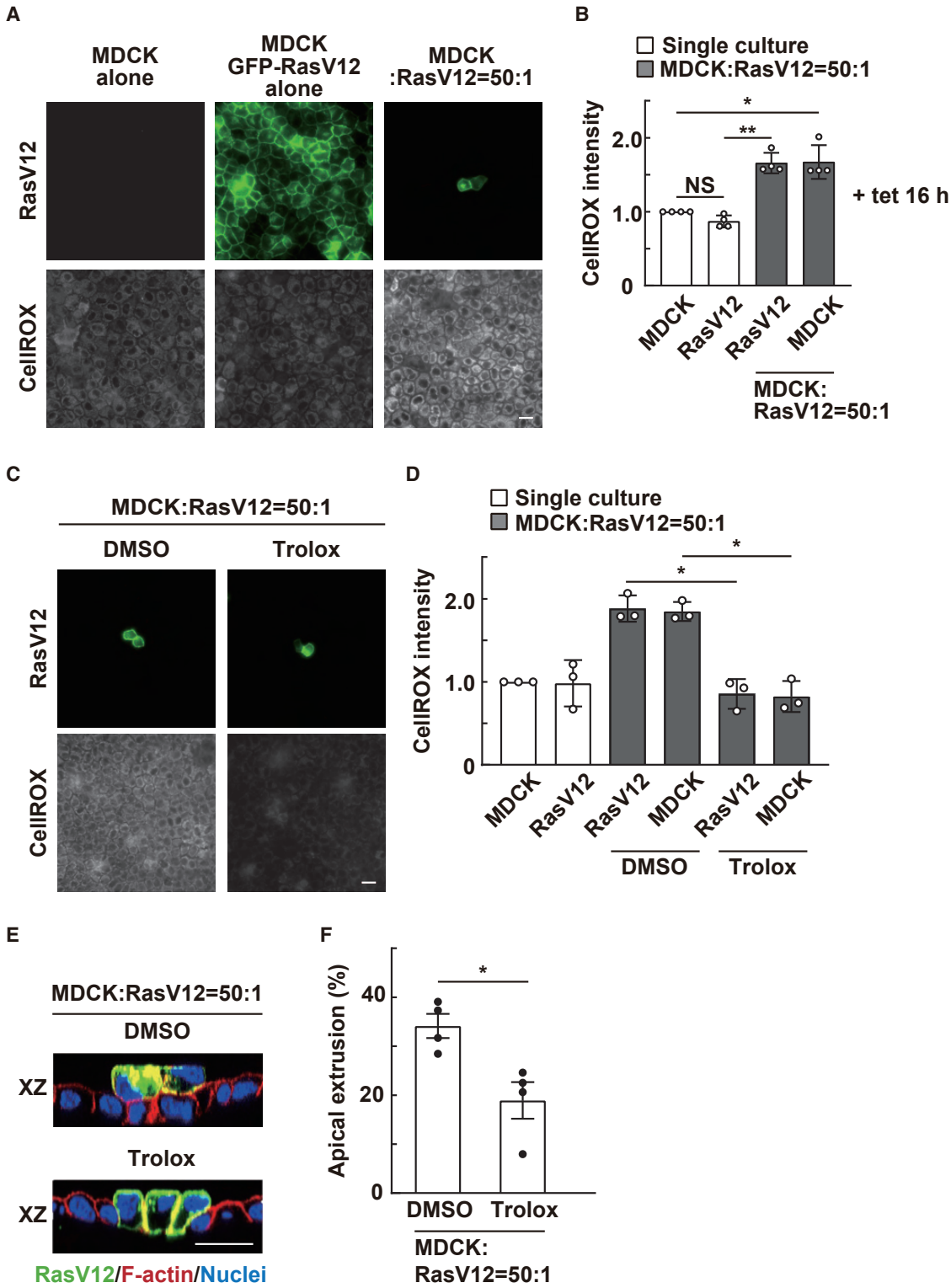

Figure 1. Upregulated ROS by the interaction of normal and RasV12-transformed cells promote apical extrusion

(A and B) The intracellular ROS levels in the single- or coculture of normal and RasV12-transformed cells. Normal MDCK cells and MDCK-pTR GFP-RasV12 cells were cultured alone or cocultured at a ratio of 50:1, and the intracellular ROS level was examined by CellROX. (A) CellROX fluorescent images. (B) Quantification of fluorescent intensity of CellROX. Values are expressed as a ratio relative to single-cultured MDCK cells. Data are mean ± SD from four independent experiments. *$p < 0.05$, **$p < 0.01$; NS, not significant (one-way ANOVA with Tukey's test); n = 373, 364, 234, and 585 cells.

(legend continued on next page)

cells, whereas the moderate level of ROS can regulate various physiological phenomena such as cell proliferation, metabolism, and motility.[34–36] In this study, we demonstrate that the extracellular ATP and ROS pathways play a prevalent role in cell extrusion.

RESULTS

The interaction between normal and RasV12- or Src-transformed cells promotes the level of ROS within an epithelial layer

A previous study using the imaginal disc epithelia of *Drosophila* demonstrated that ROS play a role in cell competition.[37] To examine the involvement of ROS in cell competition in mammals, we used CellROX Orange Reagent, a fluorogenic probe that exhibits bright orange fluorescence upon oxidation by ROS, and Madin-Darby canine kidney (MDCK) epithelial cells stably expressing GFP-RasV12 in a tetracycline-inducible manner.[19] It was previously reported that under the coculture condition of normal MDCK and RasV12-expressing MDCK cells, at 18–24 h after tetracycline addition, RasV12 cells are apically extruded from a monolayer of normal cells in a cell-death-independent manner via cell competition.[19] When normal or RasV12-transformed cells were cultured alone, the levels of intracellular ROS remained low (Figures 1A and 1B). In contrast, when normal and RasV12 cells were cocultured, the ROS levels were substantially elevated in both normal and RasV12 cells (Figures 1A and 1B). The increased ROS level was observed at 10–16 h after tetracycline addition (Figures 1B and S1A) and under various mix-ratio conditions of normal and RasV12 cells from 1:1 to 2,000:1 (Figure S1B). The increase of the ROS level in the surrounding normal cells was observed further than 160 μm (10–13 cell length) around most of the RasV12 cells (Figure S1C, left), and around some of the RasV12 cells, the ROS level was gradually decreased but retained within 160 μm (Figure S1C, right), demonstrating the increased ROS level over the wide range of surrounding normal cells. When normal and GFP-expressing cells were cocultured, the upregulation of ROS did not occur (Figures S1D and S1E). The addition of the ROS scavenger Trolox profoundly diminished the ROS levels in both normal and RasV12 cells (Figures 1C and 1D). In addition, the Trolox treatment significantly suppressed apical extrusion of RasV12-transformed cells from the epithelial monolayer (Figures 1E and 1F). The ROS levels were also elevated in the coculture of normal and Src-transformed cells (Figures S1F and S1G), and the Trolox treatment suppressed apical extrusion of Src cells (Figure S1H). Collectively, these data suggest that ROS play a crucial role in cell-competition-mediated extrusion of transformed cells.

NOX2-mediated ROS production in normal cells facilitates apical extrusion of RasV12-transformed cells

To explore an upstream regulator of ROS, we examined the effect of various chemical inhibitors on the ROS levels and apical extrusion under the coculture condition of normal and RasV12-transformed cells (Table S1). Among the tested inhibitors, the NADPH oxidase inhibitor VAS2870 significantly suppressed both the ROS level and apical extrusion (Figures 2A and 2B; Table S1). In mammals, there are seven NADPH oxidases that are membrane-bound ROS-generating enzymes: NOX1-5 and DUOX1-2. By quantitative real-time PCR analysis, the NOX2 expression in normal and RasV12 cells and the NOX4 expression in RasV12 cells were detected, whereas the expression of the other NADPH oxidases was at an undetectable or very low level (Figure S2A). To examine the functional role of NOX2 or NOX4, we established MDCK cells stably expressing NOX2-shRNA (Figure S2B) or RasV12-transformed MDCK cells stably expressing NOX2- or NOX4-shRNA (Figure S2E). NOX2 knockdown in normal cells significantly suppressed the ROS levels in both normal and neighboring RasV12 cells (Figures 2C, 2D, and S2C) and diminished the frequency of apical extrusion (Figures 2E and S2D). In contrast, the knockdown of NOX2 or NOX4 in RasV12 cells did not affect the ROS levels (Figure S2F).

In a previous study, we have shown that when RasV12 cells are surrounded by normal cells, the expression of pyruvate dehydrogenase kinase 4 (PDK4) is non-cell autonomously elevated in RasV12 cells.[38] The increased PDK4 then phosphorylates and inactivates pyruvate dehydrogenase, thereby diminishing the mitochondrial membrane potential, which positively regulates apical extrusion of RasV12 cells.[38] We showed that NOX2 knockdown in normal cells suppressed the PDK4 expression in the cocultured RasV12 cells (Figure S3A). TMRM (tetramethylrhodamine methyl ester) is a positively charged red fluorescent dye that is incorporated into active mitochondria according to the negative membrane potential gradient across their inner membranes. Using TMRM, we also demonstrated that Trolox treatment or NOX2 knockdown in normal cells profoundly restored the mitochondrial membrane potential in RasV12 cells (Figures S3B–S3E). Collectively, these data indicate that NOX2-induced ROS production in normal cells promotes the expression of PDK4 and decreases mitochondrial activity in the neighboring RasV12 cells, thereby facilitating their apical extrusion.

Extracellular ATP signaling is an upstream regulator of ROS

Previous studies have demonstrated that extracellular ATP signaling can activate NADPH oxidase and promote ROS production.[39,40] Indeed, the addition of apyrase, an ecto-ATPase (ATP-diphosphohydrolase) that degrades extracellular ATP into

(C and D) Effect of antioxidant Trolox on the intracellular ROS levels. MDCK-pTR GFP-RasV12 cells were cocultured with normal MDCK cells at a ratio of 1:50 in the absence or presence of Trolox. (C) CellROX fluorescent images. (D) Quantification of fluorescent intensity of CellROX. Values are expressed as a ratio relative to single-cultured MDCK cells. Data are mean ± SD from three independent experiments. *$p < 0.05$ (one-way ANOVA with Dunnett's test); n = 235, 260, 166, 403, 154, and 313 cells.

(E and F) Effect of antioxidant Trolox on apical extrusion of RasV12-transformed cells. (E) The xz-immunofluorescent images of MDCK-pTR GFP-RasV12 cells surrounded by normal MDCK cells in the absence or presence of Trolox. (F) Quantification of apical extrusion of RasV12-transformed cells surrounded by normal cells. Data are mean ± SD from four independent experiments. *$p < 0.05$ (paired two-tailed Student's t test); n = 523 and 524 cells.

(A, C, and E) Scale bar, 20 μm. See also Figure S1.

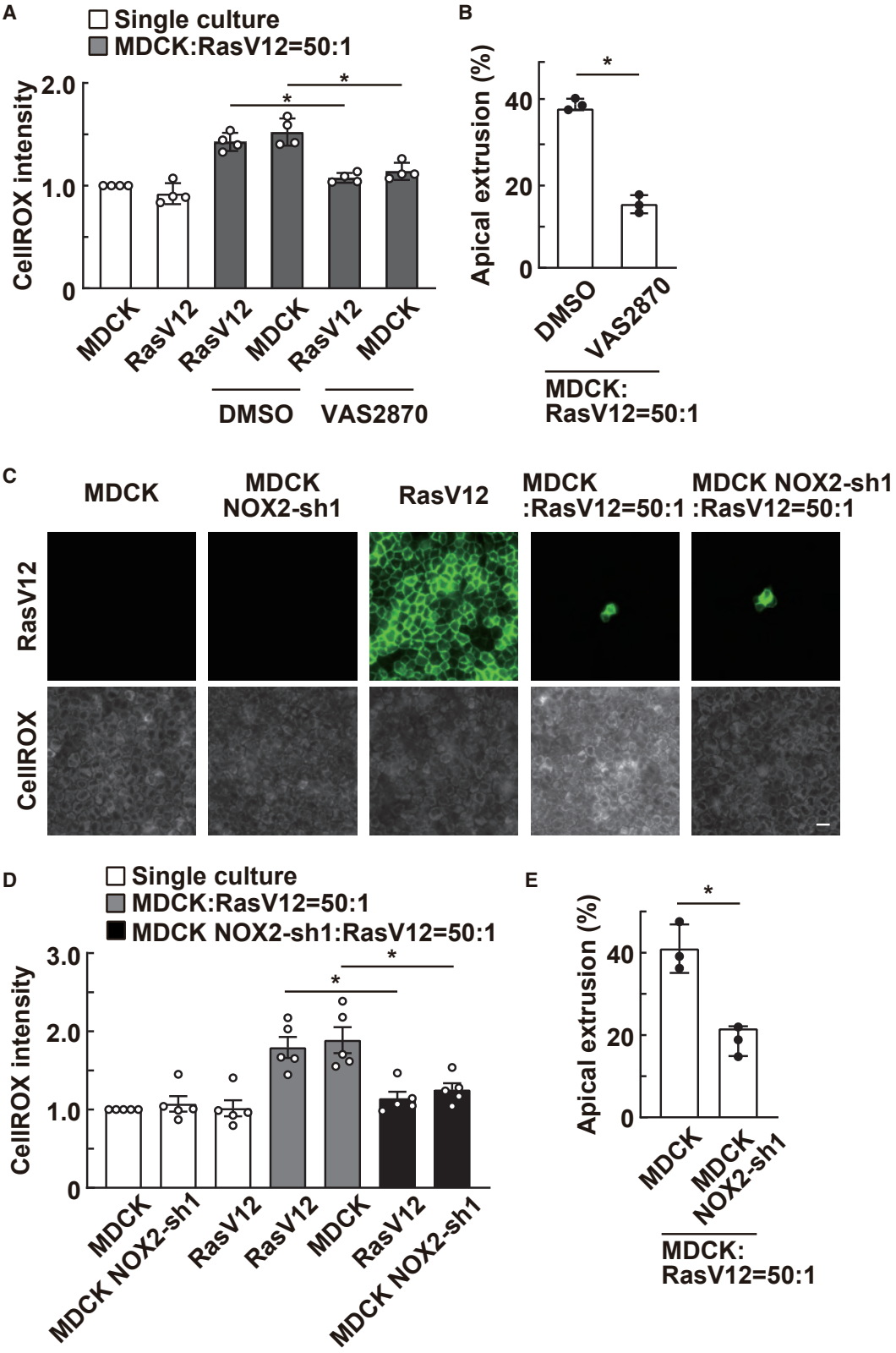

(legend on next page)

AMP significantly decreased the ROS levels in normal and RasV12-transformed cells under the mixed culture condition (Figure 3A; Table S1). Moreover, the apyrase treatment suppressed apical extrusion of RasV12 cells (Figure 3B). Extracellular ATP binds and activates purinergic P2X and P2Y receptors.[41,42] The addition of suramin, an antagonist to purinergic P2X and P2Y receptors, suppressed the ROS level and apical extrusion (Figures 3A and 3B; Table S1). To further examine extracellular ATP, we used CellTiter-Glo 2.0, a luminescent indicator for ATP. The amount of extracellular ATP in conditioned media from monocultured RasV12 cells was much higher than that from monocultured normal cells (Figure 3C). ATP can be released from the cytosol to extracellular space through multiple ATP-permeable channels: volume-regulated anion channels (VRACs), maxi-anion channels (MACs), connexin, and pannexin hemichannels.[43,44] The addition of Gd^{3+} (MACs inhibitor) or 5-Nitro-2-(3-phenylpropylamino) benzoic acid (NPPB) (inhibitor for both VRACs and MACs) reduced the extracellular ATP level in a conditioned medium from RasV12 cells (Figure S4A). In contrast, carbenoxolone (CBX) (inhibitor for both connexins and pannexins) did not affect the extracellular ATP level (Figure S4A). Furthermore, either Gd^{3+} or NPPB treatment significantly suppressed the ROS level and apical extrusion under the coculture condition (Figures S4B–S4D). We next examined the effect of exogenously added ATP in a conditioned medium. The exogenous ATP treatment increased the ROS level in normal cells but not that in NOX2-knockdown normal cells or in RasV12 cells (Figure S4E). Moreover, the ATP treatment enhanced the apical extrusion of RasV12 cells (Figure S4F). In contrast, exogenous ATP did not induce the apical extrusion of GFP cells (Figure S4F), suggesting that the activation of the extracellular ATP pathway alone is not sufficient to cause apical extrusion. Collectively, these results suggest that extracellular ATP released from RasV12 cells through MACs stimulates the production of ROS in normal cells via NOX2, which facilitates apical extrusion.

We then analyzed the expression level of purinergic P2X and P2Y receptors in normal or RasV12 cells by quantitative real-time PCR. The expression levels of most of the P2 purinergic receptors were lower in RasV12 cells than those in normal cells (Figure S4G), which may cause RasV12 cells being insensitive to extracellular ATP (Figure S4E). Among the P2Y and P2X receptors detected in this analysis, P2Y1 and P2Y2 promote the activation of NOX2.[45–47] To investigate the functional role of P2Y1 and P2Y2, we established MDCK cells stably expressing P2Y1- or P2Y2-shRNA (Figure S4H). Knockdown of either P2Y1 or P2Y2 in normal cells suppressed the ROS levels in both normal and RasV12-transformed cells under the mixed culture condition and attenuated the frequency of apical extrusion of RasV12 cells (Figures 3D, 3E, S4I, and S4J). Conversely, knockdown of NOX2 did not significantly affect the expression level of P2Y1 or P2Y2 (Figure S4G). These data suggest that extracellular ATP promotes ROS production and apical extrusion by activating P2Y1 and P2Y2 receptors in the surrounding normal cells.

Extracellular ATP and ROS pathways positively regulate apical extrusion of RasV12-transformed cells in mouse intestinal epithelia

To examine the functional role of the extracellular ATP and ROS pathways in cell extrusion *ex vivo* and *in vivo*, we used cell competition model mouse systems.[38] We crossed a *villin-Cre^{ERT2}* mouse with an *LSL-eGFP* or *LSL-Ras^{V12}-IRES-eGFP* mouse and then administrated a low dose of tamoxifen, which induced recombination events less frequently, resulting in the expression of GFP or RasV12-GFP in a mosaic manner within the intestinal epithelia. Using this system, we analyzed the fate of newly emerging RasV12-transformed cells that are surrounded by normal epithelial cells *ex vivo* and *in vivo*. First, we examined the ROS levels in intestinal organoids harboring GFP- or RasV12-expressing cells. The ROS levels were profoundly elevated in both RasV12 and surrounding normal cells within the epithelial layer in organoids harboring RasV12-expressing cells but not in organoids harboring GFP-expressing cells (Figures 4A and 4B). Moreover, antioxidant Trolox treatment significantly suppressed apical extrusion of RasV12-transformed cells from intestinal epithelia *ex vivo* (Figures 4C–4E). Furthermore, we examined the functional involvement of ROS in the apical elimination of RasV12-transformed cells *in vivo*. 4-Hydroxinonenal (4-HNE) is a product of lipid peroxidization, which is used as an oxidative stress marker. The level of 4-HNE was increased in the RasV12-expressing intestinal epithelium compared with the GFP-expressing intestine (Figure S5A). Administration of Trolox markedly suppressed the 4-HNE level and apical extrusion of RasV12 cells (Figures S5B–S5D). We further examined the functional role of extracellular ATP *ex vivo*. Apyrase treatment profoundly decreased the ROS level in intestinal organoids harboring RasV12-expressing cells (Figures 4F and 4G). Furthermore, apyrase significantly suppressed apical extrusion of RasV12 cells (Figures 4H and 4I). Collectively, these results

Figure 2. NOX2 in surrounding normal cells positively regulates ROS production, thereby promoting apical extrusion of RasV12-transformed cells

(A and B) Effect of the NADPH oxidase inhibitor VAS2870 on the intracellular ROS levels in normal or RasV12-transformed cells (A) and apical extrusion of RasV12 cells (B). (A) Quantification of fluorescent intensity of CellROX. Normal MDCK cells and MDCK-pTR GFP-RasV12 cells were cultured alone or cocultured at a ratio of 50:1 in the absence or presence of VAS2870, followed by CellROX analysis. Values are expressed as a ratio relative to single-cultured MDCK cells. Data are mean ± SD from four independent experiments. *$p < 0.05$ (one-way ANOVA with Dunnett's test); n = 175, 155, 156, 345, 130, and 272 cells.

(B) Quantification of apical extrusion of RasV12-transformed cells. Data are mean ± SD from three independent experiments. *$p < 0.05$ (paired two-tailed Student's t test); n = 377 and 416 cells.

(C and D) Effect of NOX2 knockdown in surrounding normal cells on the intracellular ROS levels. MDCK-pTR GFP-RasV12 cells were cocultured with normal MDCK cells or MDCK NOX2-shRNA1 cells at a ratio of 1:50, followed by CellROX analysis. (C) CellROX fluorescent images. Scale bar, 20 μm. (D) Quantification of fluorescent intensity of CellROX. Values are expressed as a ratio relative to single-cultured MDCK cells. Data are mean ± SD from five independent experiments. *$p < 0.05$ (one-way ANOVA with Tukey's test); n = 300, 302, 300, 279, 789, 236, and 547 cells.

(E) Effect of NOX2 knockdown in surrounding normal cells on apical extrusion of RasV12-transformed cells. Data are mean ± SD from three independent experiments. *$p < 0.05$ (paired two-tailed Student's t test); n = 324 and 299 cells.

See also Figures S2 and S3.

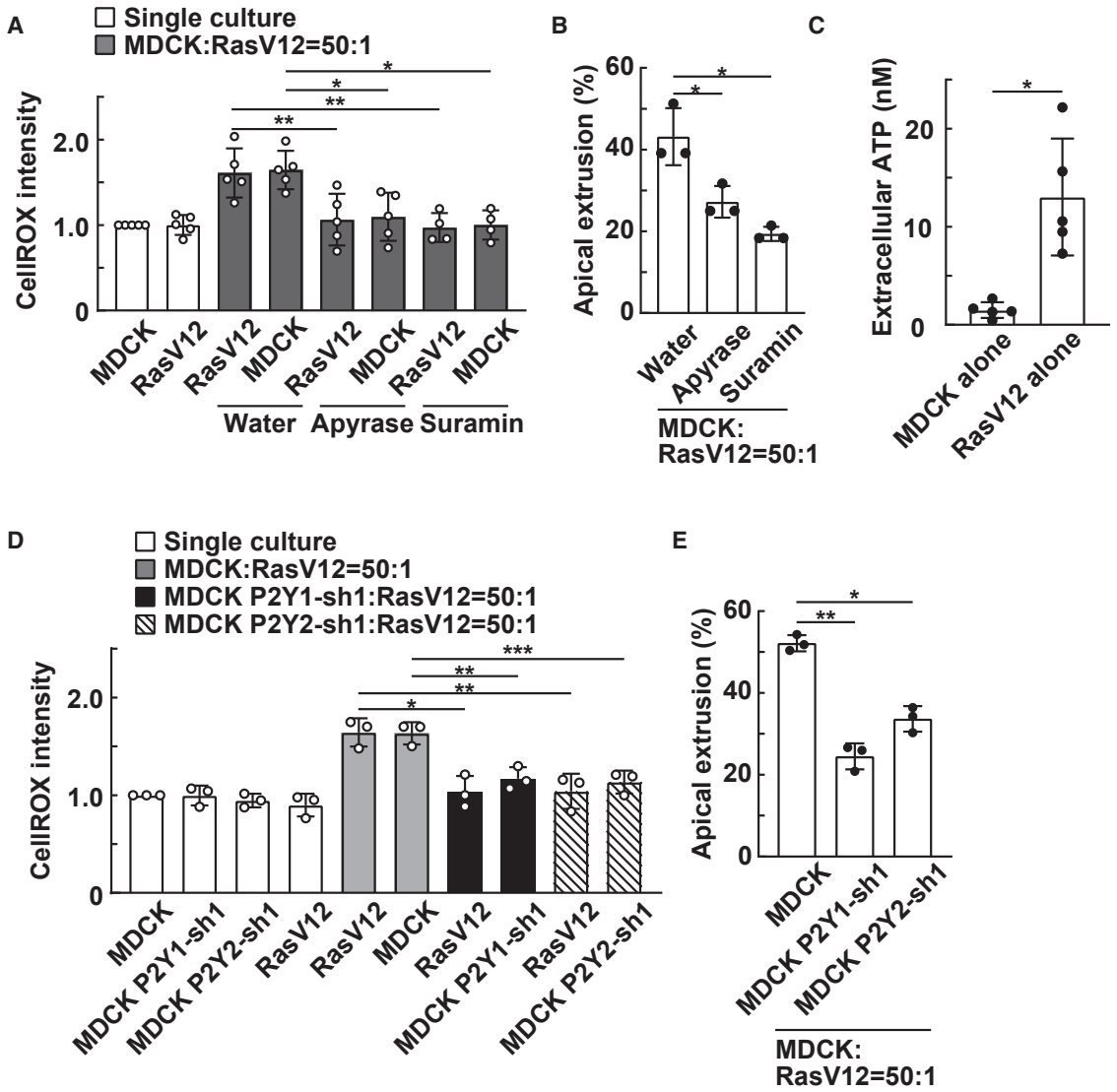

Figure 3. Extracellular ATP positively regulates the intracellular ROS level and apical extrusion

(A and B) Effect of apyrase or suramin on the intracellular ROS level (A) and apical extrusion (B).

(A) Quantification of fluorescent intensity of CellROX. Normal MDCK cells and MDCK-pTR GFP-RasV12 cells were cultured alone or cocultured at a ratio of 50:1 in the absence or presence of apyrase or suramin, followed by CellROX analysis. Values are expressed as a ratio relative to single-cultured MDCK cells. Data are mean ± SD from four (right two) or five (left six) independent experiments. *$p < 0.05$ and **$p < 0.01$ (one-way ANOVA with Dunnett's test); n = 300, 300, 328, 880, 228, 638, 206, and 556 cells.

(B) Quantification of apical extrusion of RasV12-transformed cells. Data are mean ± SD from three independent experiments. *$p < 0.05$ (one-way ANOVA with Dunnett's test); n = 327, 407, and 446 cells.

(C) Measurement of the extracellular ATP level

in conditioned media. The extracellular ATP level in conditioned media from normal MDCK or MDCK-pTR GFP-RasV12 cells cultured alone was measured using CellTite-Glo 2.0 reagent. Data are mean ± SD from five independent experiments. *$p < 0.05$ (paired two-tailed Student's t test).

(D and E) Effect of P2Y1 or P2Y2 knockdown in surrounding normal cells on the intracellular ROS levels (D) and apical extrusion (E).

(D) Quantification of fluorescent intensity of CellROX. Normal MDCK, MDCK P2Y1-shRNA1, or MDCK P2Y2-shRNA1 cells were cultured alone or cocultured with MDCK-pTR GFP-RasV12 cells at a ratio of 50:1, followed by CellROX analysis. Values are expressed as a ratio relative to single-cultured MDCK cells. Data are mean ± SD from three independent experiments. *$p < 0.05$, **$p < 0.01$, and ***$p < 0.001$ (one-way ANOVA with Dunnett's test); n = 160, 159, 149, 162, 203, 449, 140, 288, 110, and 239 cells.

(E) Quantification of apical extrusion of RasV12-transformed cells surrounded by normal, P2Y1-knockdown, or P2Y2-knockdown cells. Data are mean ± SD from three independent experiments. *$p < 0.05$ and **$p < 0.01$ (one-way ANOVA with Dunnett's test); n = 332, 361, and 335 cells.

See also Figure S4.

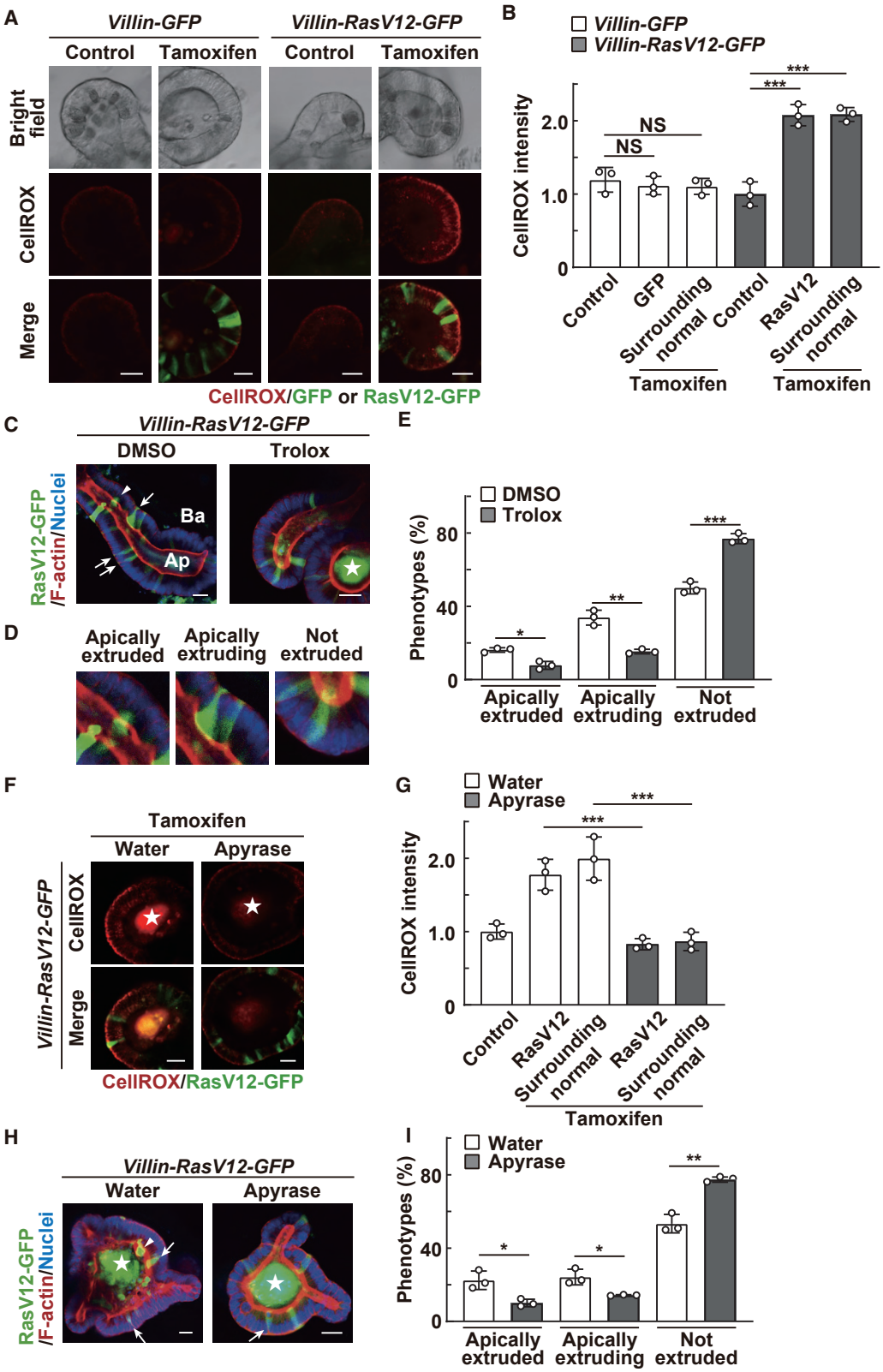

Figure 4. Extracellular ATP and ROS promote apical elimination of RasV12-transformed cells in mouse intestinal organoids

(A and B) The intracellular ROS level in mouse intestinal organoids harboring RasV12-expressing cells. Intestinal organoids from *villin-Cre^{ERT2}-LSL-eGFP* or *-LSL-Ras^{V12}-IRES-eGFP* mice were treated with 100-nM tamoxifen for 24 h, followed by CellROX analysis. (A) Fluorescent images of intestinal organoids stained with

(legend continued on next page)

indicate that extracellular ATP and ROS play a positive role in apical extrusion of RasV12-transformed cells in mouse intestinal epithelia as well.

Extracellular ATP promotes cell-competition-mediated extrusion of Scribble-knockdown cells

We next examined whether the extracellular ATP and ROS pathways also play a role in another type of cell-competition-mediated cell extrusion. When tumor suppressor protein Scribble-mutant/knockdown cells are surrounded by normal cells, cell competition occurs between these cells, and consequently, Scribble-mutant/knockdown cells undergo apoptosis and are extruded from the monolayer of normal epithelial cells.[21,22,48] When Scribble-knockdown MDCK cells were cocultured with normal MDCK cells, the ROS levels were significantly increased in both normal and Scribble-knockdown cells (Figures 5A and 5B), and Trolox treatment reduced the ROS levels (Figures 5C and 5D). In the coculture of normal and RasV12 cells, knockdown of NOX2 in normal cells suppressed the ROS level (Figures 2C and 2D). In contrast, in the coculture of normal and Scribble-knockdown cells, the ROS levels were not significantly affected by knockdown of NOX2 in normal cells (Figure S6A), suggesting that under the coculture of normal and Scribble-knockdown cells, the increase of the ROS level was induced in a NOX2-independent manner. Trolox treatment significantly suppressed the extrusion of Scribble-knockdown cells (Figure 5E), suggesting that ROS promote cell-competition-mediated extrusion of Scribble-knockdown cells. Next, we further investigated the involvement of extracellular ATP. The amount of extracellular ATP in conditioned media from monocultured Scribble-knockdown cells was higher than that from monocultured normal cells (Figure 5F). Similarly to RasV12 cells, the addition of Gd^{3+} or NPPB, but not CBX, reduced the extracellular ATP level in a conditioned medium from Scribble-knockdown cells (Figure S6B). Moreover, knockdown of P2Y1 or P2Y2 receptor in normal cells suppressed the ROS levels and extrusion of Scribble-knockdown cells under the coculture condition (Figures 5G and 5H). Collectively, these results suggest that the extracellular ATP and ROS pathways regulate both cell-death-independent and -dependent extrusion of transformed cells through cell competition.

The extracellular ATP and ROS pathways play a prevalent role in cell extrusion

Previous studies have demonstrated that cells undergoing apoptosis are apically extruded from the epithelial layer in vertebrates.[25] To explore the involvement of the extracellular ATP and ROS pathways in apoptotic cell extrusion, we established MDCK cells stably expressing GFP-tagged caspase-8 in a tetracycline-inducible manner (Figure 6A). In the coculture of normal and caspase-8-expressing cells, around 6 h after tetracycline addition, caspase-8-expressing cells underwent apoptosis and were apically extruded from the epithelial monolayer (Figure 6B). At 3 h of tetracycline treatment, membrane-impermeable SYTOX dye was not incorporated into caspase-8-expressing cells (Figure S6C), implying that membrane integrity is still maintained at this earlier time point. Under this condition, the extracellular ATP level in conditioned media from caspase-8-expressing cells was higher than that in normal cells (Figure 6C), which was diminished by treatment with apyrase or pan-caspase inhibitor Z-VAD-FMK (Figure S6D), suggesting that ATP is released from caspase-8-expressing cells at the early stage of apoptosis. We found that at 3 h of tetracycline treatment, the ROS levels were significantly increased in both normal and caspase-8-expressing cells in the coculture condition (Figures 6D and 6E). Furthermore, apyrase treatment significantly suppressed the ROS levels (Figures 6F and 6G). Furthermore, the ROS levels were also decreased by the addition of Trolox or Z-VAD-FMK (Figures 6H and 6I). Moreover, apyrase or Trolox treatment significantly prolonged the extrusion time after induction of caspase-8 expression (Figure 6J). Collectively, these data suggest that extracellular ATP and ROS also promote apoptosis-mediated cell extrusion from the epithelial layer.

CellROX. (B) Quantification of fluorescent intensity of CellROX. Values are expressed as a ratio relative to control (tamoxifen nontreated organoids). Data are mean ± SD from three independent experiments. ***$p < 0.001$; NS, not significant (one-way ANOVA with Dunnett's test); n = 122, 101, 132, 115, 90, and 136 cells.
(C–E) Effect of Trolox on apical extrusion of RasV12-expressing cells in intestinal organoids. Intestinal organoids from *villin-Cre^{ERT2}-LSL-Ras^{V12}-IRES-eGFP* mice were incubated with 100 nM tamoxifen in the absence or presence of Trolox for 24 h. (C) Immunofluorescent images of intestinal organoids harboring RasV12-expressing cells. The arrowheads or arrows indicate apically extruded or extruding RasV12-expressing cells, respectively. Ap or Ba stands for the apical or basal side of the epithelium, respectively. (D) Classification of the phenotypes of RasV12-expressing cells. "Apically extruded": completely detached from the basement membrane and translocated into the apical side. "Apically extruding": with their nucleus apically shifted but still attached to the basement membrane. "Not extruded": remaining within the epithelium. (E) Quantification of the phenotypes of RasV12-expressing cells in intestinal organoids treated with Trolox. Data are mean ± SD from three independent experiments. *$p < 0.05$, **$p < 0.01$, and ***$p < 0.001$ (unpaired two-tailed Student's t test); n = 156 (DMSO-treated organoids) or 134 (Trolox-treated organoids) cells.
(F and G) Effect of apyrase on the intracellular ROS levels in intestinal organoids harboring RasV12-expressing cells. Intestinal organoids from *villin-Cre^{ERT2}-LSL-Ras^{V12}-IRES-eGFP* mice were incubated with 100-nM tamoxifen in the absence or presence of apyrase for 24 h, followed by CellROX analysis. (F) Fluorescent images of intestinal organoids stained with CellROX after apyrase treatment. (G) Quantification of fluorescent intensity of CellROX. Values are expressed as a ratio relative to control (nontreated with tamoxifen or apyrase). Data are mean ± SD from three independent experiments. ***$p < 0.01$ (unpaired two-tailed Student's t test); n = 140, 102, 163, 73, and 123 cells.
(H and I) Effect of apyrase on apical extrusion of RasV12-transformed cells in intestinal organoids. Intestinal organoids from *villin-Cre^{ERT2}-LSL-Ras^{V12}-IRES-eGFP* mice were incubated with 100 nM tamoxifen in the absence or presence of apyrase for 24 h. (H) Immunofluorescent images of intestinal organoids treated with apyrase. The arrowhead or arrows indicate apically extruded or extruding RasV12-expressing cells, respectively. (I) Quantification of the phenotypes of RasV12-expressing cells in intestinal organoids treated with apyrase. Data are mean ± SD from three independent experiments. *$p < 0.05$ and **$p < 0.01$ (unpaired two-tailed Student's t test); n = 190 (water-treated) and 171 (apyrase-treated) cells.
(A, C, F, and H) Scale bar, 20 μm.
(C, F, and H) Stars in the images indicate mucin-rich autofluorescent materials in the apical lumen.
See also Figure S5.

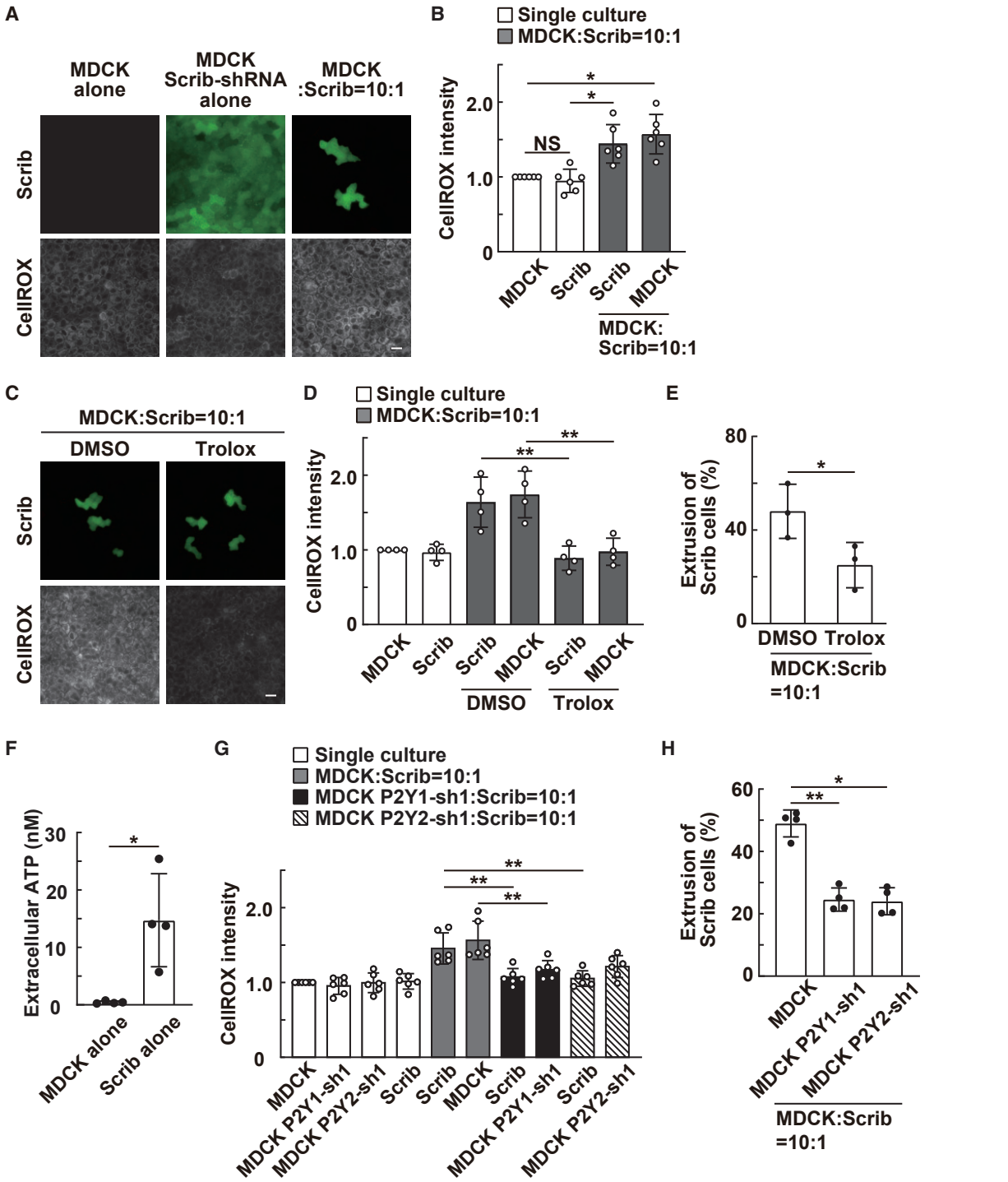

Figure 5. Extracellular ATP and ROS promote extrusion of Scribble-knockdown cells surrounded by normal cells

(A and B) The intracellular ROS levels in single- or cocultured normal and Scribble-knockdown cells. Normal MDCK cells or MDCK-pTR Scribble-shRNA1 cells were cultured alone or cocultured at a ratio of 10:1, followed by CellROX analysis. (A) CellROX fluorescent images. (B) Quantification of fluorescent intensity of CellROX. Values are expressed as a ratio relative to single-cultured MDCK cells. Data are mean ± SD from six independent experiments. *$p < 0.05$; NS, not significant (one-way ANOVA with Tukey's test); n = 355, 350, 349, and 891 cells.

(C–E) Effect of Trolox on the intracellular ROS level (C and D) and extrusion of Scribble-knockdown cells surrounded by normal cells (E).

(C) CellROX fluorescent images. MDCK-pTR Scribble-shRNA1 cells were co-cultured with normal MDCK cells at a ratio of 1:10 in the absence or presence of Trolox, followed by CellROX analysis.

(legend continued on next page)

Caspase-8-expressing cells surrounded by normal cells were often fragmented during cell extrusion, whereas single-cultured caspase-8-expressing cells were apically extruded without fragmentation (Figures S6E and S6F; Video S1). The addition of apyrase or Trolox significantly attenuated the frequency of fragmentation of caspase-8-expressing cells (Figures S6E and S6F; Videos S2 and S3). The addition of apyrase did not substantially affect the timing or intensity of the activation of downstream effector caspase-3 in the extruding cells (Figures S6G and S6H). These data imply that extracellular ATP induces the fragmentation phenotype of extruding apoptotic cells.

The extracellular ATP and ROS pathways induce directional movement of surrounding normal cells toward extruding cells

Next, we explored the functional significance of the extracellular ATP and ROS pathways in cell extrusion. During cell extrusion, the surrounding cells move toward extruding cells and fill the vacant spaces within epithelial layers, but the underlying molecular mechanism of this process remains elusive. We then analyzed the movement of surrounding cells during apical extrusion (Figure 7A); in the following experiments, we focused on the movement of the surrounding cells at the third row from extruding RasV12-transformed cells or caspase-8-expressing cells. When normal cells were cocultured with RasV12 cells, the surrounding normal cells moved further distances than normal cells cultured alone (Figure 7B; Video S4). Trolox treatment or NOX2-knockdown in normal cells significantly suppressed the increased cell motility (Figure 7B; Videos S5 and S6). Moreover, in the mixed culture condition, surrounding normal cells showed polarized movement toward extruding RasV12 cells, which was suppressed by Trolox treatment or NOX2 knockdown (Figure 7C; Videos S4, S5, and S6). We further investigated the involvement of extracellular ATP in the polarized cell movement of surrounding cells. Apyrase treatment significantly suppressed the motility and directional movement of surrounding cells toward extruding RasV12 cells (Figures 7D and 7E). Moreover, the knockdown of P2Y1 or P2Y2 receptor in normal cells also decreased the polarized movement of surrounding cells (Figures 7D and 7E). Increased cell motility and directional movement of surrounding normal cells were also observed during the extrusion of caspase-8-expressing cells (Figures 7F and 7G). Apyrase or Trolox treatment profoundly suppressed the directional movement of normal cells toward caspase-8-expressing cells (Figures 7F and 7G). Collectively, these results suggest that the extracellular ATP and ROS pathways regulate the polarized movement of the surrounding cells within the epithelial layer during cell-competition-mediated and apoptotic extrusion.

DISCUSSION

Previous studies have revealed multiple factors that are involved in the extrusion of aberrant or dysfunctional cells from epithelia. For cell-competition-mediated cell extrusion in *Drosophila* or mammals, several groups have identified membrane proteins or soluble proteins that play a key role in the interaction between loser and winner cells, including Flower, Toll-related receptors, SAS/PTP10D, EphA2, SPARC, and FGF21.[49–54] For apoptotic cell extrusion, sphingosine-1-phosphate (S1P) from apoptotic cells or surrounding environments positively regulates the delamination of apoptotic cells from the epithelial layer.[27,55] However, most of these molecules are involved in the extrusion of only certain types of cells; thus, it remains elusive whether there are common regulators that harness various types of cell extrusion. In this study, using cell culture and mouse *ex vivo* model systems, we demonstrate that extracellular ATP plays a prevalent role in cell extrusion in mammals. The blockage of the extracellular ATP signaling pathway suppresses both cell-competition-mediated extrusion and apoptotic extrusion. ATP is actively secreted from extruding cells, which profoundly influences the surrounding cells, thereby facilitating cell extrusion. Hence, extracellular ATP from extruding cells transmits the "extrude me" signal that promotes their extrusion from epithelial layers (Figure 7H). Previous studies have demonstrated that injured or infected cells secrete ATP that serves as a danger signal to recruit immune cells against tissue damage or infection.[56–58] Similarly, during the extrusion of aberrant cells from epithelial layers, extracellular ATP might act as an alerting signal to inform the neighboring cells of the presence of extruding cells to facilitate the extrusion process for the maintenance of epithelial barrier functions.

Our results suggest that Maxi-anion channel (MAC) is involved in the ATP secretion from RasV12- or Scribble-transformed cells, thereby inducing cell competition phenotypes, although we cannot exclude the possibility that ATP may be also secreted through MAC from the surrounding normal cells. The molecular identity of MAC still remains poorly understood. A recent study reported that solute carrier organic anion transporter family member 2a1 (SLCO2A1) is a key component of MAC,[59] although

(D) Quantification of fluorescent intensity of CellROX. Values are expressed as a ratio relative to single-cultured MDCK cells. Data are mean ± SD from four independent experiments. **$p < 0.01$ (one-way ANOVA with Dunnett's test); n = 235, 235, 238, 556, 209, and 458 cells.
(E) Quantification of the extrusion of Scribble-knockdown cells surrounded by normal cells after Trolox treatment. Data are mean ± SD from three independent experiments. *$p < 0.05$ (paired two-tailed Student's t test); n = 372 and 516 cells.
(F) Measurement of the extracellular ATP level
in conditioned media. The extracellular ATP level in conditioned media from normal MDCK or MDCK-pTR Scribble-shRNA1 cells cultured alone was measured using CellTite-Glo 2.0 reagent. Data are mean ± SD from four independent experiments. *$p < 0.05$ (paired two-tailed Student's t test).
(G and H) Effect of P2Y1 or P2Y2 knockdown in surrounding normal cells on the intracellular ROS level (G) and the extrusion of Scribble-knockdown cells (H).
(G) Quantification of fluorescent intensity of CellROX. MDCK-pTR Scribble-shRNA1 cells were co-cultured with normal MDCK, MDCK P2Y1-shRNA1, or MDCK P2Y2-shRNA1 cells at a ratio of 1:10, followed by CellROX analysis. Values are expressed as a ratio relative to single-cultured MDCK cells. Data are mean ± SD from six independent experiments. **$p < 0.01$ (one-way ANOVA with Dunnett's test); n = 360, 346, 350, 345, 433, 935, 391, 719, 352, and 754 cells.
(H) Quantification of the extrusion of Scribble-knockdown cells surrounded by normal, P2Y1-knockdown, or P2Y2-knockdown cells. Data are mean ± SD from four independent experiments. *$p < 0.05$ and **$p < 0.01$ (one-way ANOVA with Dunnett's test); n = 502, 723, and 716 cells.
(A and C) Scale bar, 20 μm. See also Figure S6.

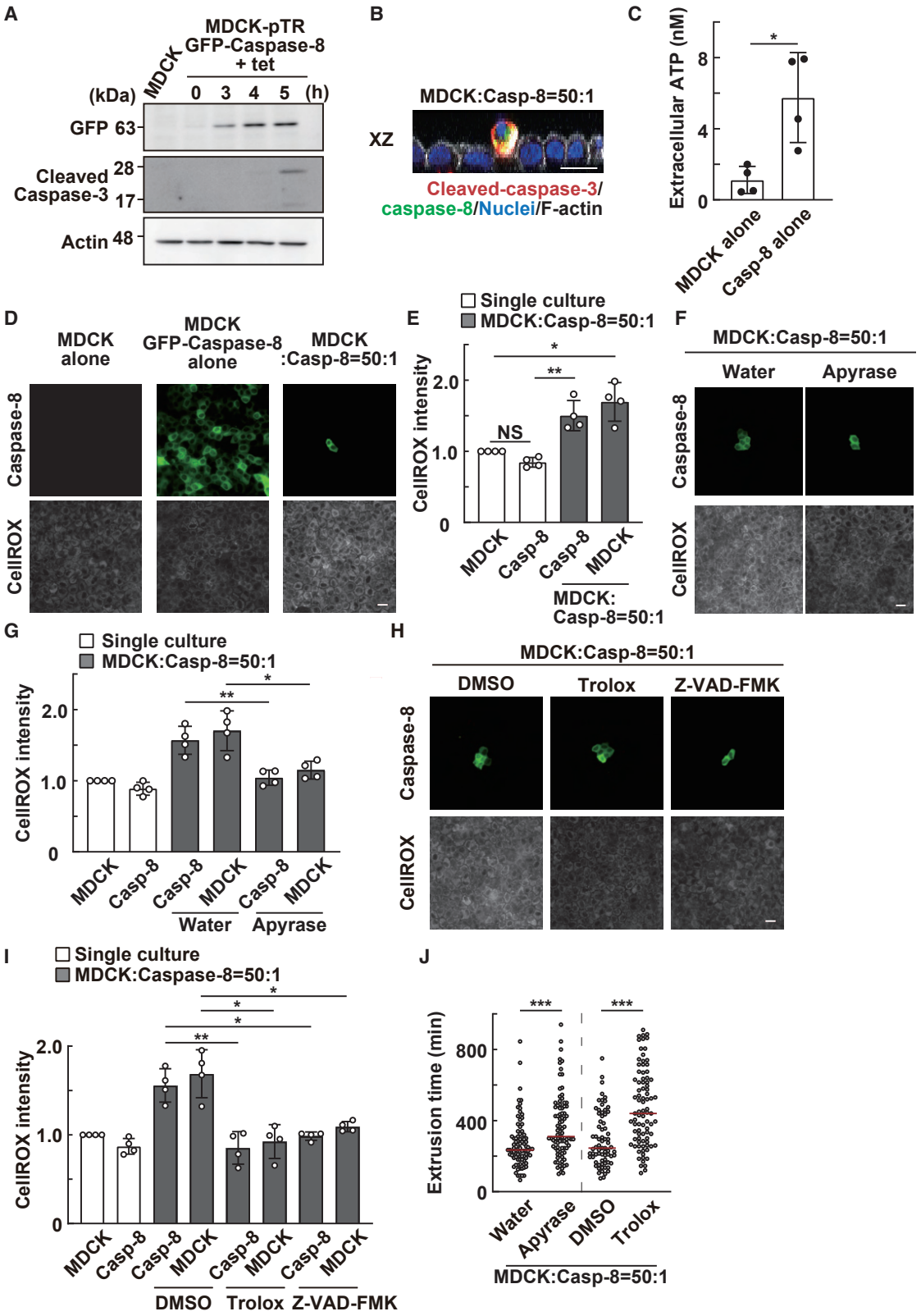

Figure 6. Extracellular ATP promotes apoptotic extrusion of caspase-8-expressing cells

(A) Establishment of a tetracycline-inducible caspase-8-expressing MDCK cell line. Tetracycline-induced expression of GFP-caspase-8 protein and the effect on the activation of downstream caspase-3 were analyzed by western blotting with the indicated antibodies.

(legend continued on next page)

the expression of SLCO2A1 is not detected in MDCK cells (data not shown). The function of MAC is silent at a steady status but can be activated by physiological or pathological stimuli such as osmotic, hypoxic, or metabolic stresses;[60–63] in particular, the relationship between MAC activity and swelling-induced stress is well documented.[61,63] Thus, it is plausible that the membrane stretching of extruding cells may trigger the ATP release. Indeed, morphological changes of transformed cells accompanying membrane stretching are observed at the early step of apical extrusion.[19] The regulatory mechanisms for extracellular ATP secretion in cell extrusion need to be further elucidated in future studies.

In this study, we have presented data indicating that ROS function downstream of the extracellular ATP signal in the extrusion of both transformed and apoptotic cells. First, treatment with apyrase or suramin, an inhibitor for extracellular ATP signaling, profoundly suppresses the ROS level within an epithelial layer. Second, the knockdown of P2Y1 or P2Y2, a receptor for extracellular ATP, also decreases the ROS level. Third, exogenously added ATP increases intracellular ROS. Furthermore, we have also revealed the molecular mechanism of how ROS positively regulate cell extrusion. Inhibition of the ROS pathway significantly suppresses the motility of surrounding cells, suggesting that the increased ROS induce the directional movement of surrounding cells toward extruding cells and promote cell extrusion by generating compressive forces onto extruding cells, consistent with previous studies that ROS positively regulate polarized cell motility.[34,64–66] Moreover, the knockdown of NOX2 in the surrounding cells also affects the mitochondrial activity in extruding transformed cells. Collectively, these data indicate that the increased ROS within the epithelial layer profoundly influence the behavior of both extruding cells and the surrounding cells, thereby regulating cell extrusion in an orchestrated manner. It is plausible, however, that other downstream regulator(s) of extracellular ATP than ROS may also play a certain role in cell extrusion.

Currently, several questions remain to be answered. First, how do ROS propagate across a wide range of the epithelial layer around extruding cells? Around most of extruding cells, the CellROX fluorescence intensity is comparable between the proximal and distant surrounding cells. Thus, diffusion of extracellular ATP alone may not be sufficient to cause the rather homogenous ROS elevation across the epithelial layer. Moreover, an inhibitor for Gap junction or Aquaporin, which potentially blocks intercellular diffusion of ROS, does not affect the ROS level, suggesting that the propagation of ROS within the epithelial layer is not mediated solely by simple diffusion of ROS. Furthermore, exosome inhibitor does not affect the ROS level either (Table S1). Thus, it remains unknown how ROS are propagated in the extracellular or intercellular spaces. Second, does the increased ROS in extruding cells play a certain role in cell extrusion? Knockdown of NOX2 in the surrounding cells diminishes the ROS level in RasV12 cells, but knockdown of NOX2 or NOX4 in RasV12 cells does not, suggesting that the increased ROS in RasV12 cells are derived from the neighboring cells. To understand the significance of elevated ROS in RasV12 cells, we have tried to establish RasV12 cell lines stably expressing a key antioxidant regulator Nrf2 but failed possibly due to the cytotoxic effect of Nrf2 overexpression. Third, is there any functional link between the extracellular ATP and ROS pathways and other regulators for cell extrusion? Calcium wave and actomyosin ring formation play a vital role in the execution of cell extrusion.[25,26] At the final step of cell extrusion, calcium wave propagates from extruding cells across the surrounding cells, which induces the formation of actomyosin rings around extruding cells, thereby generating physical forces required for cell extrusion.[26] As the increased ROS level within the epithelial layer are observed at the earlier time point (Figure S6I), it is possible that the extracellular ATP and ROS pathways act upstream of calcium wave or that extracellular ATP regulates both ROS and calcium wave in parallel. In addition to calcium wave, ERK activity waves are also generated around RasV12-expressing cells, which promote the extrusion process.[67] The MEK inhibitor U0126 does not affect the ROS level under the mixed culture condition (Table S1), indicating that ERK waves do not act upstream of ROS, but there remains a possibility that secreted extracellular ATP from transformed cells may trigger ERK waves. These issues need to be clarified in future studies.

Various types of aberrant cells can be extruded from epithelial layers, including damaged, dysfunctional, transformed, infected,

(B) Representative image of apically extruded caspase-8-expressing cells from an epithelial layer of normal cells. MDCK-pTR GFP-caspase-8 cells were cocultured with normal MDCK cells at a ratio of 1:50, followed by tetracycline treatment for 6 h.

(C) Measurement of the extracellular ATP level
in conditioned media. The extracellular ATP level in conditioned media from normal MDCK or MDCK-pTR GFP-caspase-8 cells cultured alone was measured using CellTiter-Glo 2.0 reagent. Data are mean ± SD from four independent experiments. *$p < 0.05$ (paired two-tailed Student's t test).

(D and E) The intracellular ROS levels in single- or cocultured normal and caspase-8-expressing cells. Normal MDCK cells and MDCK-pTR GFP-caspase-8 cells were cultured alone or cocultured at a ratio of 50:1, followed by CellROX analysis. (D) CellROX fluorescent images. (E) Quantification of fluorescent intensity of CellROX. Values are expressed as a ratio relative to single-cultured MDCK cells. Data are mean ± SD from four independent experiments. *$p < 0.05$, **$p < 0.01$; NS, not significant (one-way ANOVA with Tukey's test); n = 240, 230, 157, and 456 cells.

(F–I) Effect of apyrase, Trolox, or Z-VAD-FMK on the intracellular ROS levels in cocultured normal and caspase-8-expressing cells. Normal MDCK cells and MDCK-pTR GFP-caspase-8 cells were cultured alone or cocultured at a ratio of 50:1 in the absence or presence of apyrase (F and G), Trolox, or Z-VAD-FMK (H and I), followed by CellROX analysis.

(F and H) CellROX fluorescent images.

(G and I) Quantification of fluorescent intensity of CellROX. Values are expressed as a ratio relative to single-cultured MDCK cells. Data are mean ± SD from four independent experiments. *$p < 0.05$ and **$p < 0.01$ (one-way ANOVA with Dunnett's test); (G) n = 240, 230, 151, 401, 155, and 385 cells; (I) n = 230, 220, 149, 394, 161, 347, 169, and 368 cells.

(J) Effect of apyrase or Trolox on extrusion time of caspase-8-expressing cells. MDCK-pTR GFP-caspase-8 cells were cocultured with normal MDCK cells at a ratio of 1:50 in the absence or presence of apyrase or Trolox. Red bars indicate median values. ***$p < 0.001$ (Mann-Whitney test); n = 87, 89, 72, and 87 cells from two independent experiments.

(B, D, F, and H) Scale bar, 20 μm. See also Figure S6.

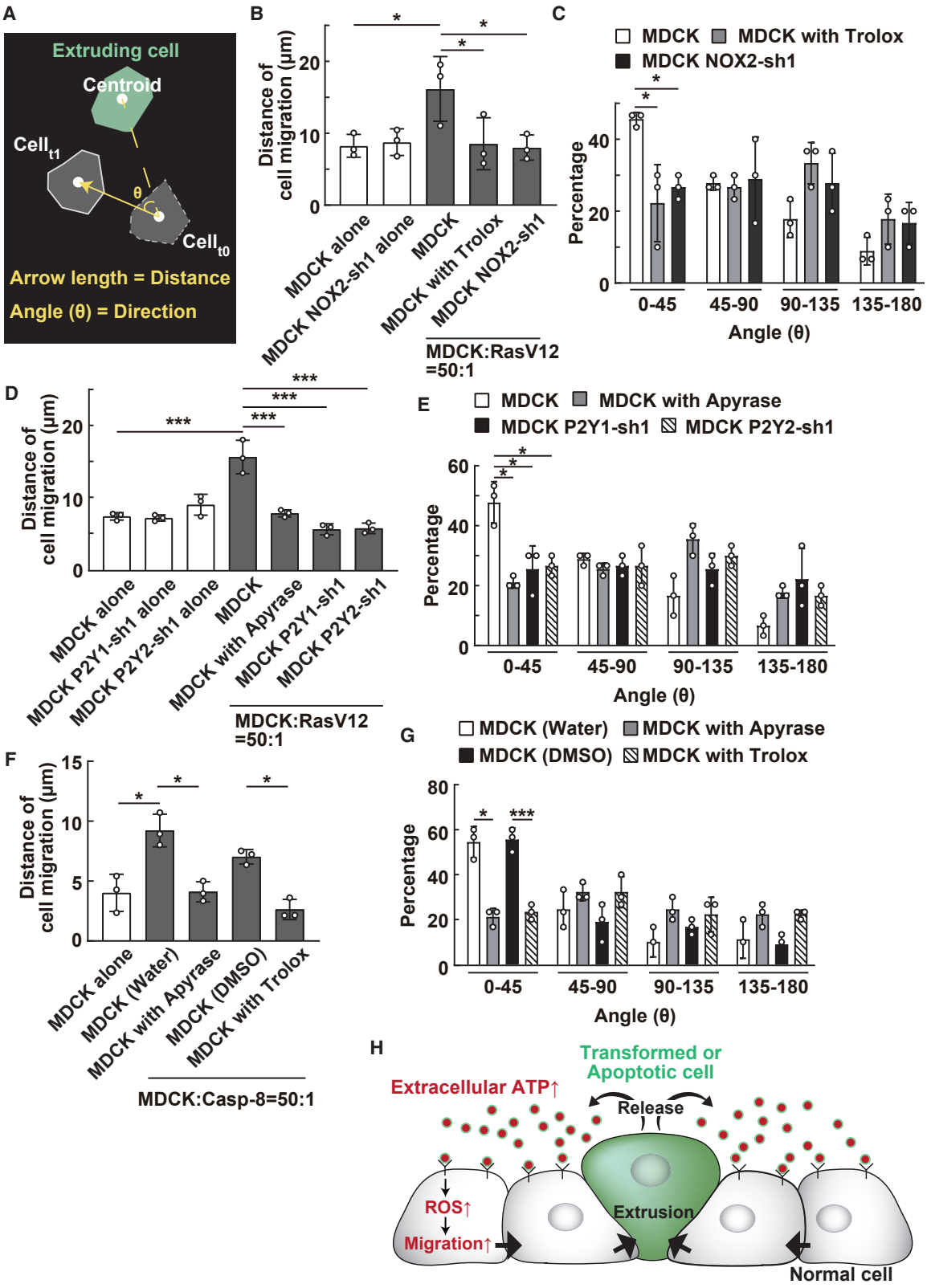

Figure 7. Extracellular ATP and ROS promote directional movement of surrounding normal cells toward extruding cells

(A) Analysis of distance and direction of cell migration. The schematic for the directional movement of surrounding cells toward extruding cells. The yellow arrow denotes the movement of a surrounding cell. Angle (θ) is measured between two lines: a solid line linking the centroids of a surrounding cell at the start and end of

(legend continued on next page)

aged, and dead cells.[1–4,68,69] Previous studies have demonstrated that the extrusion/removal of aberrant cells is required for proper embryonic development and also prevents aging and tissue degeneration in the adult.[68,70–72] Thus, the dysregulation of cell extrusion processes would potentially cause a variety of pathological conditions or disorders by accumulating abnormal or harmful cells within epithelial tissues. Hence, the further elucidation of molecular mechanisms for cell extrusion could lead to clinical applications for the maintenance of tissue homeostasis and the improvement of human health.

STAR★METHODS

Detailed methods are provided in the online version of this paper and include the following:

- KEY RESOURCES TABLE
- RESOURCE AVAILABILITY
  - Lead contact
  - Materials availability
  - Data and code availability
- EXPERIMENTAL MODEL AND SUBJECT DETAILS
  - Cell line
  - Animal model
- METHOD DETAILS
  - Antibodies and materials
  - Establishment of cell lines and cell culture
  - Immunofluorescence and western blotting
  - Time-lapse observation of cultured cells
  - Quantitative real-time PCR
  - Measurement of the extracellular ATP level
  - Mice
- QUANTIFICATION AND STATICAL ANALYSIS
  - Statistics analysis

SUPPLEMENTAL INFORMATION

Supplemental information can be found online at https://doi.org/10.1016/j.cub.2022.03.057.

ACKNOWLEDGMENTS

We acknowledge support from Japan Society for the Promotion of Science (JSPS) grant-in-aid for Scientific Research on Transformative Research 21H05285A01, grant-in-aid for Scientific Research (S) 21H05039, JSPS Bilateral Joint Research Projects (the Royal Society) JPJSBP1 20215703, JSPS grant-in-aid for Challenging Research (Pioneering) 20K21411, Japan Science and Technology Agency (JST) (Moonshot R&D: grant number JPMJPS2022), the Takeda Science Foundation, and SAN-ESU GIKEN CO. LTD (to Y.F.); JSPS grant-in-aid for Transformative Research Areas (A) (21H05287) (to T.I.); and JST SPRING (grant number JPMJSP2110) (to Y.M.). This work was also supported by Kyoto University Live Imaging Center.

AUTHOR CONTRIBUTIONS

Y.M. designed experiments and generated most of the data. N. Shiratsuchi, N. Sato, A.C., N.T., S.I., M.K., I.K., S.K., Y.H., and T.I. assisted with experiments. Y.F. conceived and designed the study. The manuscript was written by Y.M., N. Shiratsuchi, and Y.F. with assistance from the other authors.

DECLARATION OF INTERESTS

The authors declare no competing interests.

Received: December 9, 2021
Revised: February 28, 2022
Accepted: March 18, 2022
Published: April 12, 2022

REFERENCES

1. Mitchell, S.J., and Rosenblatt, J. (2021). Early mechanical selection of cell extrusion and extrusion signaling in cancer. Curr. Opin. Cell Biol. *72*, 36–40.
2. Villars, A., and Levayer, R. (2022). Collective effects in epithelial cell death and cell extrusion. Curr. Opin. Genet. Dev. *72*, 8–14.
3. Gudipaty, S.A., and Rosenblatt, J. (2017). Epithelial cell extrusion: pathways and pathologies. Semin. Cell Dev. Biol. *67*, 132–140.
4. Ohsawa, S., Vaughen, J., and Igaki, T. (2018). Cell extrusion: a stress-responsive force for good or evil in epithelial homeostasis. Dev. Cell *44*, 532.
5. Katoh, H., and Fujita, Y. (2012). Epithelial homeostasis: elimination by live cell extrusion. Curr. Biol. *22*, R453–R455.

the observation (t0 and t1) and a dashed line linking the centroid of a surrounding and extruding cell at t0. Arrow length and angle indicate the distance and direction of the cell movement, respectively.
(B and C) Effect of Trolox or NOX2 knockdown on the migration of normal cells surrounding RasV12-transformed cell. Normal MDCK cells or MDCK NOX2-shRNA1 cells were cultured alone or cocultured with MDCK-pTR GFP-RasV12 cells at a ratio of 50:1 in the absence or presence of Trolox.
(B) Total distance of migration of normal cells or NOX2-knockdown cells for 6 h. Data are mean ± SD from three independent experiments. *$p < 0.05$ (one-way ANOVA with Dunnett's test); n = 90 cells for all conditions.
(C) Analysis of directional movement of normal cells or NOX2-knockdown cells toward RasV12-transformed cells. Data are mean ± SD from three independent experiments. *$p < 0.05$ (one-way ANOVA with Dunnett's test); n = 90 cells for all conditions.
(D and E) Effect of inhibition of extracellular ATP signaling on the migration of normal cells toward RasV12-transformed cell. Normal MDCK, MDCK P2Y1-shRNA1, or MDCK P2Y2-shRNA1 cells were cultured alone or cocultured with MDCK-pTR GFP-RasV12 cells at a ratio of 50:1 in the absence or presence of apyrase.
(D) The total distance of cell migration of normal cells, P2Y1-knockdown, or P2Y2-knockdown cells for 6 h. Data are mean ± SD from three independent experiments. ***$p < 0.001$ (one-way ANOVA with Dunnett's test); n = 90 cells for all conditions.
(E) Analysis of directional movement of normal cells, P2Y1-knockdown, or P2Y2-knockdown cells toward RasV12-transformed cells. Data are mean ± SD from three independent experiments. *$p < 0.05$ (one-way ANOVA with Dunnett's test); n = 90 cells for all conditions.
(F and G) Effect of inhibition of the extracellular ATP and ROS pathways on the migration of normal cells toward caspase-8-expressing cells. Normal MDCK cells were cultured alone or cocultured with MDCK-pTR GFP-caspase-8 cells at a ratio of 50:1 in the absence or presence of apyrase or Trolox.
(F) Total distance of migration of normal cells for 2 h. Data are mean ± SD from three independent experiments. *$p < 0.05$ (one-way ANOVA with Tukey's test); n = 90 cells for all conditions.
(G) Analysis of directional movement of normal cells toward caspase-8-expressing cells in the absence or presence of apyrase or Trolox. Data are mean ± SD from three independent experiments. *$p < 0.05$ and ***$p < 0.001$ (unpaired two-tailed Student's t test); n = 90 cells for all conditions.
(H) A schematic model of cell extrusion induced by extracellular ATP and ROS pathways.

6. Amoyel, M., and Bach, E.A. (2014). Cell competition: how to eliminate your neighbours. Development *141*, 988–1000.
7. Johnston, L.A. (2009). Competitive interactions between cells: death, growth, and geography. Science *324*, 1679–1682.
8. Vishwakarma, M., and Piddini, E. (2020). Outcompeting cancer. Nat. Rev. Cancer *20*, 187–198.
9. Morata, G., and Calleja, M. (2020). Cell competition and tumorigenesis in the imaginal discs of Drosophila. Semin. Cancer Biol. *63*, 19–26.
10. Bowling, S., Lawlor, K., and Rodríguez, T.A. (2019). Cell competition: the winners and losers of fitness selection. Development *146*, dev167486.
11. Díaz-Díaz, C., and Torres, M. (2019). Insights into the quantitative and dynamic aspects of cell competition. Curr. Opin. Cell Biol. *60*, 68–74.
12. Madan, E., Gogna, R., and Moreno, E. (2018). Cell competition in development: information from flies and vertebrates. Curr. Opin. Cell Biol. *55*, 150–157.
13. Maruyama, T., and Fujita, Y. (2017). Cell competition in mammals - novel homeostatic machinery for embryonic development and cancer prevention. Curr. Opin. Cell Biol. *48*, 106–112.
14. Baker, N.E. (2020). Emerging mechanisms of cell competition. Nat. Rev. Genet. *21*, 683–697.
15. Levayer, R. (2020). Solid stress, competition for space and cancer: the opposing roles of mechanical cell competition in tumour initiation and growth. Semin. Cancer Biol. *63*, 69–80.
16. Kajita, M., Sugimura, K., Ohoka, A., Burden, J., Suganuma, H., Ikegawa, M., Shimada, T., Kitamura, T., Shindoh, M., Ishikawa, S., et al. (2014). Filamin acts as a key regulator in epithelial defence against transformed cells. Nat. Commun. *5*, 4428.
17. Kon, S., and Fujita, Y. (2021). Cell competition-induced apical elimination of transformed cells, EDAC, orchestrates the cellular homeostasis. Dev. Biol. *476*, 112–116.
18. Kajita, M., Hogan, C., Harris, A.R., Dupre-Crochet, S., Itasaki, N., Kawakami, K., Charras, G., Tada, M., and Fujita, Y. (2010). Interaction with surrounding normal epithelial cells influences signalling pathways and behaviour of Src-transformed cells. J. Cell Sci. *123*, 171–180.
19. Hogan, C., Dupré-Crochet, S., Norman, M., Kajita, M., Zimmermann, C., Pelling, A.E., Piddini, E., Baena-López, L.A., Vincent, J.P., Itoh, Y., et al. (2009). Characterization of the interface between normal and transformed epithelial cells. Nat. Cell Biol. *11*, 460–467.
20. Leung, C.T., and Brugge, J.S. (2012). Outgrowth of single oncogene-expressing cells from suppressive epithelial environments. Nature *482*, 410–413.
21. Norman, M., Wisniewska, K.A., Lawrenson, K., Garcia-Miranda, P., Tada, M., Kajita, M., Mano, H., Ishikawa, S., Ikegawa, M., Shimada, T., et al. (2012). Loss of Scribble causes cell competition in mammalian cells. J. Cell Sci. *125*, 59–66.
22. Brumby, A.M., and Richardson, H.E. (2003). Scribble mutants cooperate with oncogenic Ras or Notch to cause neoplastic overgrowth in Drosophila. EMBO J. *22*, 5769–5779.
23. Grzeschik, N.A., Amin, N., Secombe, J., Brumby, A.M., and Richardson, H.E. (2007). Abnormalities in cell proliferation and apico-basal cell polarity are separable in Drosophila lgl mutant clones in the developing eye. Dev. Biol. *311*, 106–123.
24. Igaki, T., Pagliarini, R.A., and Xu, T. (2006). Loss of cell polarity drives tumor growth and invasion through JNK activation in Drosophila. Curr. Biol. *16*, 1139–1146.
25. Rosenblatt, J., Raff, M.C., and Cramer, L.P. (2001). An epithelial cell destined for apoptosis signals its neighbors to extrude it by an actin- and myosin-dependent mechanism. Curr. Biol. *11*, 1847–1857.
26. Takeuchi, Y., Narumi, R., Akiyama, R., Vitiello, E., Shirai, T., Tanimura, N., Kuromiya, K., Ishikawa, S., Kajita, M., Tada, M., et al. (2020). Calcium wave promotes cell extrusion. Curr. Biol. *30*, 670–681.e6.
27. Duszyc, K., Gomez, G.A., Lagendijk, A.K., Yau, M.K., Nanavati, B.N., Gliddon, B.L., Hall, T.E., Verma, S., Hogan, B.M., Pitson, S.M., et al. (2021). Mechanotransduction activates RhoA in the neighbors of apoptotic epithelial cells to engage apical extrusion. Curr. Biol. *31*, 1326–1336.e5.
28. Valon, L., Davidović, A., Levillayer, F., Villars, A., Chouly, M., Cerqueira-Campos, F., and Levayer, R. (2021). Robustness of epithelial sealing is an emerging property of local ERK feedback driven by cell elimination. Dev. Cell *56*, 1700–1711.e8.
29. Gerasimovskaya, E.V., Ahmad, S., White, C.W., Jones, P.L., Carpenter, T.C., and Stenmark, K.R. (2002). Extracellular ATP is an autocrine/paracrine regulator of hypoxia-induced adventitial fibroblast growth. Signaling through extracellular signal-regulated kinase-1/2 and the Egr-1 transcription factor. J. Biol. Chem. *277*, 44638–44650.
30. Elliott, M.R., Chekeni, F.B., Trampont, P.C., Lazarowski, E.R., Kadl, A., Walk, S.F., Park, D., Woodson, R.I., Ostankovich, M., Sharma, P., et al. (2009). Nucleotides released by apoptotic cells act as a find-me signal to promote phagocytic clearance. Nature *461*, 282–286.
31. Idzko, M., Ferrari, D., and Eltzschig, H.K. (2014). Nucleotide signalling during inflammation. Nature *509*, 310–317.
32. Faas, M.M., Sáez, T., and de Vos, P. (2017). Extracellular ATP and adenosine: the Yin and Yang in immune responses? Mol. Aspects Med. *55*, 9–19.
33. Schwiebert, E.M., and Zsembery, A. (2003). Extracellular ATP as a signaling molecule for epithelial cells. Biochim. Biophys. Acta. *1615*, 7–32.
34. Hurd, T.R., DeGennaro, M., and Lehmann, R. (2012). Redox regulation of cell migration and adhesion. Trends Cell Biol. *22*, 107–115.
35. Sies, H., and Jones, D.P. (2020). Reactive oxygen species (ROS) as pleiotropic physiological signalling agents. Nat. Rev. Mol. Cell Biol. *21*, 363–383.
36. Forrester, S.J., Kikuchi, D.S., Hernandes, M.S., Xu, Q., and Griendling, K.K. (2018). Reactive oxygen species in metabolic and inflammatory signaling. Circ. Res. *122*, 877–902.
37. Kucinski, I., Dinan, M., Kolahgar, G., and Piddini, E. (2017). Chronic activation of JNK JAK/STAT and oxidative stress signalling causes the loser cell status. Nat. Commun. *8*, 136.
38. Kon, S., Ishibashi, K., Katoh, H., Kitamoto, S., Shirai, T., Tanaka, S., Kajita, M., Ishikawa, S., Yamauchi, H., Yako, Y., et al. (2017). Cell competition with normal epithelial cells promotes apical extrusion of transformed cells through metabolic changes. Nat. Cell Biol. *19*, 530–541.
39. Dichmann, S., Idzko, M., Zimpfer, U., Hofmann, C., Ferrari, D., Luttmann, W., Virchow, C., Jr., Di Virgilio, F., and Norgauer, J. (2000). Adenosine triphosphate-induced oxygen radical production and CD11b up-regulation: Ca(++) mobilization and actin reorganization in human eosinophils. Blood *95*, 973–978.
40. Pines, A., Perrone, L., Bivi, N., Romanello, M., Damante, G., Gulisano, M., Kelley, M.R., Quadrifoglio, F., and Tell, G. (2005). Activation of APE1/Ref-1 is dependent on reactive oxygen species generated after purinergic receptor stimulation by ATP. Nucleic Acids Res. *33*, 4379–4394.
41. Di Virgilio, F., Chiozzi, P., Ferrari, D., Falzoni, S., Sanz, J.M., Morelli, A., Torboli, M., Bolognesi, G., and Baricordi, O.R. (2001). Nucleotide receptors: an emerging family of regulatory molecules in blood cells. Blood *97*, 587–600.
42. Ralevic, V., and Burnstock, G. (1998). Receptors for purines and pyrimidines. Pharmacol. Rev. *50*, 413–492.
43. Sabirov, R.Z., and Okada, Y. (2005). ATP release via anion channels. Purinergic Signal. *1*, 311–328.
44. Chekeni, F.B., Elliott, M.R., Sandilos, J.K., Walk, S.F., Kinchen, J.M., Lazarowski, E.R., Armstrong, A.J., Penuela, S., Laird, D.W., Salvesen, G.S., et al. (2010). Pannexin 1 channels mediate 'find-me' signal release and membrane permeability during apoptosis. Nature *467*, 863–867.
45. Díaz-Vegas, A., Campos, C.A., Contreras-Ferrat, A., Casas, M., Buvinic, S., Jaimovich, E., and Espinosa, A. (2015). ROS production via P2Y1-PKC-NOX2 is triggered by extracellular ATP after electrical stimulation of skeletal muscle cells. PLoS ONE *10*, e0129882.
46. Sudi, S.B., Tanaka, T., Oda, S., Nishiyama, K., Nishimura, A., Sunggip, C., Mangmool, S., Numaga-Tomita, T., and Nishida, M. (2019). TRPC3-Nox2

axis mediates nutritional deficiency-induced cardiomyocyte atrophy. Sci. Rep. *9*, 9785.

47. Cheng, S.E., Lee, I.T., Lin, C.C., Wu, W.L., Hsiao, L.D., and Yang, C.M. (2013). ATP mediates NADPH oxidase/ROS generation and COX-2/PGE2 expression in A549 cells: role of P2 receptor-dependent STAT3 activation. PLoS ONE *8*, e54125.
48. Igaki, T., Pastor-Pareja, J.C., Aonuma, H., Miura, M., and Xu, T. (2009). Intrinsic tumor suppression and epithelial maintenance by endocytic activation of Eiger/TNF signaling in Drosophila. Dev. Cell *16*, 458–465.
49. Rhiner, C., López-Gay, J.M., Soldini, D., Casas-Tinto, S., Martín, F.A., Lombardía, L., and Moreno, E. (2010). Flower forms an extracellular code that reveals the fitness of a cell to its neighbors in Drosophila. Dev. Cell *18*, 985–998.
50. Yamamoto, M., Ohsawa, S., Kunimasa, K., and Igaki, T. (2017). The ligand Sas and its receptor PTP10D drive tumour-suppressive cell competition. Nature *542*, 246–250.
51. Meyer, S.N., Amoyel, M., Bergantiños, C., de la Cova, C., Schertel, C., Basler, K., and Johnston, L.A. (2014). An ancient defense system eliminates unfit cells from developing tissues during cell competition. Science *346*, 1258236.
52. Porazinski, S., de Navascués, J., Yako, Y., Hill, W., Jones, M.R., Maddison, R., Fujita, Y., and Hogan, C. (2016). EphA2 drives the segregation of Ras-transformed epithelial cells from normal neighbors. Curr. Biol. *26*, 3220–3229.
53. Portela, M., Casas-Tinto, S., Rhiner, C., López-Gay, J.M., Domínguez, O., Soldini, D., and Moreno, E. (2010). Drosophila SPARC is a self-protective signal expressed by loser cells during cell competition. Dev. Cell *19*, 562–573.
54. Ogawa, M., Kawarazaki, Y., Fujita, Y., Naguro, I., and Ichijo, H. (2021). FGF21 induced by the ASK1-p38 pathway promotes mechanical cell competition by attracting cells. Curr. Biol. *31*, 1048–1057.e5.
55. Gu, Y., Forostyan, T., Sabbadini, R., and Rosenblatt, J. (2011). Epithelial cell extrusion requires the sphingosine-1-phosphate receptor 2 pathway. J. Cell Biol. *193*, 667–676.
56. Kouzaki, H., Iijima, K., Kobayashi, T., O'Grady, S.M., and Kita, H. (2011). The danger signal, extracellular ATP, is a sensor for an airborne allergen and triggers IL-33 release and innate Th2-type responses. J. Immunol. *186*, 4375–4387.
57. Sáez, P.J., Vargas, P., Shoji, K.F., Harcha, P.A., Lennon-Duménil, A.M., and Sáez, J.C. (2017). ATP promotes the fast migration of dendritic cells through the activity of pannexin 1 channels and P2X7 receptors. Sci. Signal. *10*.
58. Idzko, M., Hammad, H., van Nimwegen, M., Kool, M., Willart, M.A., Muskens, F., Hoogsteden, H.C., Luttmann, W., Ferrari, D., Di Virgilio, F., et al. (2007). Extracellular ATP triggers and maintains asthmatic airway inflammation by activating dendritic cells. Nat. Med. *13*, 913–919.
59. Sabirov, R.Z., Merzlyak, P.G., Okada, T., Islam, M.R., Uramoto, H., Mori, T., Makino, Y., Matsuura, H., Xie, Y., and Okada, Y. (2017). The organic anion transporter SLCO2A1 constitutes the core component of the Maxi-Cl channel. EMBO J. *36*, 3309–3324.
60. Liu, H.T., Tashmukhamedov, B.A., Inoue, H., Okada, Y., and Sabirov, R.Z. (2006). Roles of two types of anion channels in glutamate release from mouse astrocytes under ischemic or osmotic stress. Glia *54*, 343–357.
61. Liu, H.T., Toychiev, A.H., Takahashi, N., Sabirov, R.Z., and Okada, Y. (2008). Maxi-anion channel as a candidate pathway for osmosensitive ATP release from mouse astrocytes in primary culture. Cell Res. *18*, 558–565.
62. Liu, H.T., Sabirov, R.Z., and Okada, Y. (2008). Oxygen-glucose deprivation induces ATP release via maxi-anion channels in astrocytes. Purinergic Signal. *4*, 147–154.
63. Sabirov, R.Z., and Okada, Y. (2009). The maxi-anion channel: a classical channel playing novel roles through an unidentified molecular entity. J. Physiol. Sci. *59*, 3–21.
64. Ushio-Fukai, M. (2006). Localizing NADPH oxidase-derived ROS. Sci. STKE *2006*, re8.
65. Moldovan, L., Moldovan, N.I., Sohn, R.H., Parikh, S.A., and Goldschmidt-Clermont, P.J. (2000). Redox changes of cultured endothelial cells and actin dynamics. Circ. Res. *86*, 549–557.
66. Wu, R.F., Gu, Y., Xu, Y.C., Nwariaku, F.E., and Terada, L.S. (2003). Vascular endothelial growth factor causes translocation of p47phox to membrane ruffles through WAVE1. J. Biol. Chem. *278*, 36830–36840.
67. Aikin, T.J., Peterson, A.F., Pokrass, M.J., Clark, H.R., and Regot, S. (2020). MAPK activity dynamics regulate non-cell autonomous effects of oncogene expression. eLife *9*, e60541.
68. Liu, N., Matsumura, H., Kato, T., Ichinose, S., Takada, A., Namiki, T., Asakawa, K., Morinaga, H., Mohri, Y., De Arcangelis, A., et al. (2019). Stem cell competition orchestrates skin homeostasis and ageing. Nature *568*, 344–350.
69. Bastounis, E.E., Serrano-Alcalde, F., Radhakrishnan, P., Engström, P., Gómez-Benito, M.J., Oswald, M.S., Yeh, Y.T., Smith, J.G., Welch, M.D., García-Aznar, J.M., et al. (2021). Mechanical competition triggered by innate immune signaling drives the collective extrusion of bacterially infected epithelial cells. Dev. Cell *56*, 443–460.e11.
70. Akieda, Y., Ogamino, S., Furuie, H., Ishitani, S., Akiyoshi, R., Nogami, J., Masuda, T., Shimizu, N., Ohkawa, Y., and Ishitani, T. (2019). Cell competition corrects noisy Wnt morphogen gradients to achieve robust patterning in the zebrafish embryo. Nat. Commun. *10*, 4710.
71. Hashimoto, M., and Sasaki, H. (2019). Epiblast formation by TEAD-YAP-dependent expression of pluripotency factors and competitive elimination of unspecified cells. Dev. Cell *50*, 139–154.e5.
72. Merino, M.M., Rhiner, C., Lopez-Gay, J.M., Buechel, D., Hauert, B., and Moreno, E. (2015). Elimination of unfit cells maintains tissue health and prolongs lifespan. Cell *160*, 461–476.
73. Ohoka, A., Kajita, M., Ikenouchi, J., Yako, Y., Kitamoto, S., Kon, S., Ikegawa, M., Shimada, T., Ishikawa, S., and Fujita, Y. (2015). EPLIN is a crucial regulator for extrusion of RasV12-transformed cells. J. Cell Sci. *128*, 781–789.
74. Hogan, C., Serpente, N., Cogram, P., Hosking, C.R., Bialucha, C.U., Feller, S.M., Braga, V.M., Birchmeier, W., and Fujita, Y. (2004). Rap1 regulates the formation of E-cadherin-based cell-cell contacts. Mol. Cell. Biol. *24*, 6690–6700.

STAR★METHODS

KEY RESOURCES TABLE

REAGENT or RESOURCE	SOURCE	IDENTIFIER
Antibodies		
Rabbit anti-Cleaved Caspase-3 antibody (Asp175)	Cell Signaling Technology	Cat# 9661; RRID: AB_2341188
Mouse anti-Actin antibody (clone C4)	Merk Millipore	Cat# MAB1501
Mouse anti-GFP antibody	Sigma-Aldrich	Cat# 11814460001; RRID: AB_390913
Chicken anti-GFP antibody	Abcam	Cat# ab13970; RRID: AB_300798
Rabbit anti-4-hydroxynonenal antibody	Abcam	Cat# ab46545; RRID: AB_722490
Rat anti-E-cadherin antibody	Life technologies	Cat# 13–1900; RRID: AB_2533005
Horseradish peroxidase-conjugated AffiniPure anti-mouse IgG	Jakson ImmunoResearch	Cat# 715-035-151
Horseradish peroxidase-conjugated AffiniPure anti-rabbit IgG	Jakson ImmunoResearch	Cat# 711-035-152
Alexa Fluor 488 Anti-chicken	Thermo Fisher	Cat# A11039; RRID: AB_142924
Alexa Fluor 568 Anti-rabbit	Thermo Fisher	Cat# A21069; RRID: AB_10563601
Alexa Fluor 647 Anti-rat	Thermo Fisher	Cat# 51-4031-80; RRID: AB_823213
Alexa Fluor-568-conjugated phalloidin	Life technologies	Cat# A12380
Alexa Fluor-647-conjugated phalloidin	Life technologies	Cat# 22287
Chemicals, peptides, and recombinant proteins		
Z-VAD-FMK	Calbiochem	Cat# 219007
(S)-(-)-blebbistatin	Calbiochem	Cat# 203391
LY294002	Calbiochem	Cat# 440204
CK666	Calbiochem	Cat# 182515
SMIFH2	Calbiochem	Cat# 44092
Y27632	Calbiochem	Cat# 688000
ibuprofen	Sigma-Aldrich	Cat# I4883
CCCP	Sigma-Aldrich	Cat# C2759
a-Glycyrrhetinic acid	Sigma-Aldrich	Cat# G8053
Silver nitrate	Sigma-Aldrich	Cat# S6506
apyrase	Sigma-Aldrich	Cat# A7646
Carbenoxolone disodium salt	Sigma-Aldrich	Cat# C4790
VAS2870	Sigma-Aldrich	Cat# SML0273
BAPTA-AM	Sigma-Aldrich	Cat# A1076
5-Nitro-2-(3-3 phenylpropylamino) benzoic acid	Sigma-Aldrich	Cat# N4779
Gadolinium (III) chloride hexahydrate	Sigma-Aldrich	Cat# 203289
GW4869	Sigma-Aldrich	Cat# D1692
nocodazole	Sigma-Aldrich	Cat# M1404
ATP disodium salt hydrate	Sigma-Aldrich	Cat# A2383
Trolox	Sigma-Aldrich	Cat# 238813
Trolox	Cayman Chemical	Cat# 10011659
H-89 dihydrochloride	Cayman Chemical	Cat# 10010556
BAY117082	Santa Cruz Biotechnology	Cat# sc-200615B
Suramin sodium	Santa Cruz Biotechnology	Cat# sc-200833
ML141	Santa Cruz Biotechnology	Cat# 4266
U0126	Promega	Cat# V1121
GsMTx	PEPTIDE INSTITUTE	Cat# 4393-S
Blasticidin	InvivoGen	Cat# ant-bl

(*Continued on next page*)

Continued

REAGENT or RESOURCE	SOURCE	IDENTIFIER
Zeocin	InvivoGen	Cat# ant-zn-5
G418 (Geneticin)	GIBCO	Cat# 10131027
tetracycline	Sigma-Aldrich	Cat# T7660
Tamoxifen	Sigma-Aldrich	Cat# T5648
Cell Recovery Solution	Corning	Cat# 354253
FSC 22 Clear Frozen Section Compound	Leica Biosystems	Cat# 3801480
Matrigel	Corning	Cat# 356231
Type I collagen (Cellmatrix Type I-A)	Nitta Gelatin	N/A
Type I collagen (Cellmatrix Type I-P)	Nitta Gelatin	N/A
Hoechst 33342	Life Technologies	Cat# H3570
Critical commercial assays		
CellTiter-Glo 2.0	Promega	Cat# G9241
QuantiTect Reverse Transcription	Qiagen	Cat# 205311
MycoAlart	Lonza	Cat# LT07-118
GeneAce SYBR qPCR Mix	NIPPON GENE	Cat# 319-07683
Nucview 530 Caspase-3 substrate	Biotium	Cat# 10406
SiR-actin Kit (far-red silicon rhodamine (SiR)-actin fluorescence probe)	SPIROCHROME	Cat# CY-SC001
SYTOX Orange Nucleic Acid Stain	Thermo Fisher Scientific	Cat# S11368
TMRM	Thermo Fisher Scientific	Cat# T668
CellROX orange	Thermo Fisher Scientific	Cat# C10443
Trizol	Thermo Fisher Scientific	Cat# 15596018
Experimental models: Cell lines		
MDCK	Dr. W. Birchmeier	N/A
Experimental models: Organisms/strains		
Mouse: *Villin/Cre^{ERT2}; LoxP-STOP-LoxP /eGFP*	[38]	N/A
Mouse: *Villin/Cre^{ERT2}; LoxP-STOP-LoxP / HRasV12-IRES-eGFP*	[38]	N/A
Oligonucleotides		
See Table S2	N/A	N/A
Recombinant DNA		
pcDNA4-TO-eGFP-human-caspase-8	This paper	N/A
Software and algorithms		
Metamorph	Molecular Devices	ht.tps://www.moleculardevices.co.jp/systems/metamorph-microscopy-automation-and-image-analysis-software
ImageJ	NHI Image	https://imagej.nih.gov/ij/download.html
GraphPad Prism 7	GraphPad Software	https://www.mdf-soft.com/products/graphpad_prism8.html

RESOURCE AVAILABILITY

Lead contact

Further information and requests for resources and reagents should be directed to and will be fulfilled by the lead contact, Yasuyuki Fujita (fujita@monc.med.kyoto-u.ac.jp).

Materials availability

Plasmids or cell lines generated in this study will be made available on request, but we may require payment and/or a completed Materials Transfer Agreement if there is potential for commercial application.

Data and code availability

- Data reported in this paper will be shared by the lead contact upon request.
- This paper does not report the original code.
- Any additional information required to reanalyze the data reported in this paper is available from the lead contact upon request.

EXPERIMENTAL MODEL AND SUBJECT DETAILS

Cell line

MDCK (Madin-Darby canine kidney) cells were cultured in Dulbecco's modified Eagle's medium (DMEM) supplemented with 10% fetal bovine serum (FBS) (Sigma-Aldrich), 1% penicillin/streptomycin (Life Technologies), and 1% GlutaMax (Life Technologies) in a humidified 5% CO2 incubator at 37°C. The parental MDCK cells were a gift from W. Birchmeier (MDC, Berlin). Mycoplasma contamination was regularly tested for all cell lines using MycoAlert Mycoplasma Detection kit (Lonza).

Animal model

All animal experiments were conducted under the guidelines of the Animal Care Committee of Kyoto University. The animal protocols were reviewed and approved by the Animal Research Committee of Graduate School of Medicine, Kyoto University (MedKyo21059). 6-12-week old *villin/Cre^{ERT}; LoxP-STOP-LoxP (LSL)/HRas^{V12}-IRES-eGFP* (a C57BL/6 genetic background) and *villin/Cre^{ERT}; LSL/eGFP* mice (a C57BL/6 genetic background) of either sex were used in this study. All mice were bred and/or maintained under a 14 h light /10 h dark cycle with food and water available at all times at the Institute of Laboratory Animals, Graduate School of Medicine, Kyoto University.

METHOD DETAILS

Antibodies and materials

Rabbit anti-Cleaved Caspase-3 (Asp175) (#9661) antibody was purchased from Cell Signaling Technology. Mouse anti-β-actin (MAB1501R clone C4) and mouse anti-GFP (#11814460001) (used for western blotting) antibodies were from Merck Millipore. Chicken anti-GFP (ab13970) (used for immunohistochemistry) and rabbit anti-4-hydroxynonenal (ab46545) antibodies were from Abcam. Rat anti-E-cadherin (131900) antibody was from Life Technologies. Horseradish peroxidase-conjugated AffiniPure anti-mouse and anti-rabbit IgG were from Jackson ImmunoResearch. Alexa-Fluor-568-conjugated phalloidin (Life Technologies) was used at 1.0 unit/mL. Alexa-Fluor-488-, -568-, and -647-conjugated secondary antibodies were from Life Technologies. Hoechst 33342 (Life Technologies) was used at a dilution of 1:5,000. The inhibitors Z-VAD-FMK (100 μM), CK666 (100 μM), (S)-(-)-blebbistatin (30 μM), LY294002 (10 μM), Y27632 (20 μM), and SMIFH2 (25 μM) were from Calbiochem. CCCP (5 μM), ibuprofen (10 μM), α-Glycyrrhetinic acid (α-GA; 50 μM), silver nitrate (50 μM), apyrase (1 unit/mL), carbenoxolone disodium salt (50 μM), VAS2870 (1 μM), BAPTA-AM (25 μM), 5-Nitro-2-(3-phenylpropylamino)benzoic acid (NPPB; 50 μM), Gadolinium (III) chloride hexahydrate (10 μM), GW4869 (20 μM), and nocodazole (200 μg/mL) were from Sigma-Aldrich. Trolox (1 mM) and H-89 dihydrochloride (20 μM) were from Cayman Chemical. BAY117082 (1 μM), suramin sodium (10 μM), and ML141 (20 μM) were from Santa Cruz Biotechnology. U0126 (10 μM) was from Promega. GsMTx (10 μM) was from PEPTIDE INSTITUTE. ATP disodium salt hydrate (1 mM) was from Sigma-Aldrich. Type I collagen (Cellmatrix Type I-A and Cellmatrix Type I-P) was obtained from Nitta Gelatin and was neutralized on ice according to the manufacturer's instructions. The SiR-actin Kit (far-red silicon rhodamine (SiR)-actin fluorescence probe) was obtained from SPIROCHROME to stain F-actin and was used according to the manufacturer's instructions.

Establishment of cell lines and cell culture

MDCK cells stably expressing GFP (MDCK-pTR GFP), GFP-RasV12 (MDCK-pTR GFP-RasV12), GFP-cSrcY527F (MDCK-pTR GFP-SrcY527F), or Scribble-short hairpin RNA (shRNA) (MDCK-pTR Scribble-shRNA1) in a tetracycline-inducible manner were established and cultured as previously described.[19,21,73] To establish MDCK-pTR GFP-caspase-8 cells, MDCK-pTR cells were transfected with pcDNA4/TO/eGFP-human-caspase-8 by nucleofection using Nucleofector 2b (Lonza), followed by selection in the medium containing 5 μg/mL of blasticidin (Invitrogen) and 400 μg/mL of zeocin (Invitrogen). To establish MDCK cells stably expressing NOX2-shRNA, P2Y1-shRNA, P2Y2-shRNA, or luciferase-shRNA as well as MDCK-pTR GFP-RasV12 cells stably expressing NOX2-shRNA or NOX4-shRNA, each shRNA oligonucleotide was cloned into BglII/XhoI sites of pSUPER.neo (Oligoengine). Sequences of shRNA oligonucleotides are shown in Table S2. MDCK cells were transfected with pSUPER.neo-NOX2-shRNA, -P2Y1-shRNA, -P2Y2-shRNA, or -luciferase-shRNA by nucleofection, followed by selection in the medium containing 800 μg/mL of Geneticin (G418; Gibco). MDCK-pTR GFP-RasV12 cells were transfected with pSUPER.neo-NOX2-shRNA or -NOX4-shRNA by nucleofection, followed by selection in the medium containing 5 μg/mL of blasticidin, 400 μg/mL of zeocin, and 800 μg/mL of G418. For tetracycline-inducible MDCK cell lines, 2 μg/mL of tetracycline (Sigma-Aldrich) was used to induce the expression of proteins or shRNAs.

Immunofluorescence and western blotting

For immunofluorescence analysis, MDCK, MDCK NOX2-shRNA, MDCK P2Y1-shRNA, MDCK P2Y2-shRNA, or MDCK luciferase-shRNA cells were mixed with MDCK-pTR GFP-RasV12, MDCK-pTR GFP-cSrcY527F, or MDCK-pTR GFP-caspase-8 cells at a ratio of 50:1 and plated onto collagen-coated coverslips as previously described.[19] The mixture of cells was incubated for 8-12 h, followed by tetracycline treatment for 24 h, except for the analysis of extrusion of SrcY527F-transformed cells or caspase-8-expressing cells, in which cells were examined at 18 h or 6 h after tetracycline treatment, respectively. The indicated inhibitor was added together with tetracycline. After incubation with tetracycline, cells were fixed with 4% paraformaldehyde (PFA) in phosphate-buffered saline (PBS) and permeabilized as previously described.[18] For immunofluorescence using intestinal organoids, cells grown in matrigels were incubated with Cell Recovery Solution (Corning) for 8 min before fixation with 4% PFA. After fixation, cells were permeabilized in 0.5% Triton X-100/PBS for 1 h and incubated with 1% bovine serum albumin (BSA)/PBS for 1 h. For immunohistochemical analysis of the small intestine, mice were perfused with 1% PFA. The isolated tissues were fixed with 1% PFA in PBS for 24 h and embedded in FSC 22 Clear Frozen Section Compound (Leica Biosystems). 10-mm-thick frozen sections were cut using Leica CM3050S cryostat (Leica Biosystems). The sections were incubated with 1 x Block-Ace (DS Pharma Biomedical) and 0.1% Triton X-100 in PBS for 1 h, followed by incubation with primary or secondary antibody diluted in PBS containing 0.1 x Block-Ace and 0.1% TritonX-100 for 2 h or 1 h respectively at room temperature. All primary antibodies were used at 1:100 except for mouse intestinal tissues: anti-GFP (1:1,000), anti-E-cadherin (1:2,000), and anti-4-hydroxynonenal (1:100) antibodies. All secondary antibodies were used at 1:200 for cultured cells and 1:1,000 for mouse intestinal tissues, respectively. Immunofluorescence images were analyzed with Olympus FV1000 or FV1200 using the Olympus FV10-ASW software. Images were quantified with the MetaMorph software (Molecular Devices) and the Image J software. To monitor the intracellular ROS level in cultured cells, MDCK-pTR GFP, MDCK-pTR GFP-RasV12, MDCK-pTR GFP-cSrcY527F, MDCK-pTR Scribble-shRNA1, or MDCK-pTR GFP-caspase-8 cells were mixed with non-transformed MDCK cells and plated on collagen-coated 35-mm glass-bottom dishes and cultured for 8-12 h, followed by addition of tetracycline. Inhibitors were added together with tetracycline. For the inhibition of apoptosis, cells were treated with Z-VAD-FMK for 2 h before tetracycline addition. At 3 h (for caspase-8 cells), 12 h (for SrcY527F cells), 16 h (for RasV12 cells and GFP cells), or 36 h (for Scribble-knockdown cells) after tetracycline addition, cells were incubated with 5 μM CellROX (Invitrogen) for 30 min according to the manufacturer's instructions. After labeling, images of twelve randomly selected fields (2,048 x 2,048 pixels) were captured using a phase-contrast microscope. To monitor the mitochondrial membrane potential, cells were loaded with 50 nM TMRM (Thermo Fisher Scientific) for 30 min and observed as previously described.[38] For Figure S6C, to monitor the membrane integrity of cultured cells, 1.0 x 10^6 MDCK cells or MDCK-pTR GFP-caspase-8 cells were seeded on collagen-coated 35-mm glass-bottom dishes and cultured for 8-12 h, followed by the treatment of tetracycline for 3 or 6 h. Cells were then incubated with 0.5 μM SYTOX Orange Nucleic Acid Stain (Thermo Fisher Scientific) for 10 min, and images were captured as described above. Western blotting was performed as previously described.[74] Primary and secondary antibodies were used at 1:1,000. Western blotting data were analyzed using ImageQuant LAS4010 (GE healthcare).

Time-lapse observation of cultured cells

For live-cell imaging, cells were incubated in the Leibovitz's L-15 medium (Gibco) containing 10% FBS. Time-lapse images were captured and analyzed by Nikon confocal microscopy (A1 HD25) with the NIS-Elements software (Nikon). Acquired data were analyzed by the Image J software. For the analysis of the cell movement around RasV12 cells, 5.0 x 10^5 MDCK, MDCK NOX2-shRNA1, MDCK P2Y1-shRNA1, or MDCK P2Y2-shRNA1 cells were co-cultured with MDCK-pTR GFP-RasV12 cells at a ratio of 50:1 on the collagen-coated 35-mm glass-bottom dishes for 6 h. Cells were then cultured in the medium containing the far-red silicon rhodamine (SiR)-actin fluorescence probes for 24 h until time-lapse observation started. Tetracycline was added to the medium 8 h before the start of time-lapse imaging. Time-lapse imaging was performed for 6 h to examine the cell movement. For the analysis of the effect of Trolox or apyrase on the cell movement, the inhibitor was added together with tetracycline. Cell movement was measured by tracking the centroids of surrounding cells every hour, and the cumulative distance for 6 h was shown as total distance of cell migration. The angle of directional movement of surrounding cells was calculated based on centroids of RasV12-transformed cells and surrounding cells as demonstrated in Figure 7A. For the analysis of apoptotic cell extrusion, 8.0 x 10^4 MDCK cells were cocultured with MDCK-pTR GFP-caspase-8 cells at a ratio of 50:1 on the collagen-coated 8-well glass-bottom plates (Thermo Fisher Scientific) for 8-16 h. The indicated inhibitor and tetracycline were then added together to the medium. After 2 h of the inhibitor and tetracycline addition, apoptotic cell extrusion was analyzed by time-lapse imaging for 24 h. For analyses of the extrusion time of caspase-8-expressing cells, the time zero was defined as the time when the GFP intensity exceeded 1.1 times as the background fluorescence intensity. Fragmentation of caspase-8-expressing cells upon extrusion was determined using bright-field images of time-lapse observation. For the analysis of the cell movement around caspase-8-expressing cells, surrounding cells were analyzed for 2 h until membrane blebbing was observed in caspase-8-expressing cells. For the analysis of extrusion of Scribble-knockdown cells, 4.0 x 10^5 MDCK, MDCK P2Y1-shRNA1, or MDCK P2Y2-shRNA1 cells were co-cultured with MDCK-pTR Scribble-shRNA1 cells at a ratio of 10:1 on the collagen-coated 35-mm glass-bottom dishes for 8 h. Cells were then treated with tetracycline for 36 h. After 36 h of tetracycline treatment, time-lapse analysis was performed for 24 h. For the analysis of the effect of Trolox on the extrusion of Scribble-knockdown cells, Trolox was added into culture media after 24 h of tetracycline treatment. Extrusion of Scribble-knockdown cells was determined by the obvious morphological change using bright-field images. To monitor the activity of caspase-3 in cultured cells in live imaging, MDCK cells were co-cultured with MDCK-pTR GFP-caspase-8 cells at a ratio of 50:1 on the collagen-coated 8-well glass-bottom dishes for 8-16 h. Nucview 530 Caspase-3 substrate (2 μM) (Biotium) was then added together with tetracycline and apyrase. After 2 h of the treatment, the activity of caspase-3 was analyzed by time-lapse imaging for 24 h.

Quantitative real-time PCR

For quantitative real-time PCR, the indicated cells were seeded at a density of 1×10^6 cells on a 6-well plate (Corning). After incubation with tetracycline for 16 h, total RNA was extracted using TRIzol (Thermo Fisher Scientific) and reverse transcribed using QuantiTect Reverse Transcription (Qiagen). qPCR reactions were performed with GeneAce SYBR qPCR Mix (NIPPON GENE) using the StepOne system (Thermo Fisher Scientific). For the analysis of the *PDK4* expression in RasV12-transformed cells, 2 $x10^7$ MDCK or MDCK NOX2-shRNA1 cells were mixed with MDCK-pTR GFP-RasV12 cells at a ratio of 10:1 and seeded on collagen-coated 15-cm dishes (Greiner-Bio-One) as previously described.[38] After incubation with tetracycline for 16 h, GFP-positive RasV12 cells and GFP-negative MDCK cells were separated using an analytical flow cytometer (SH800S, SONY). Relative quantification analysis was performed with the comparative CT method ($2^{-\Delta\Delta CT}$) using β-*actin* as a reference gene to normalize data. The primer sequences are shown in Table S2.

Measurement of the extracellular ATP level

For the measurement of the extracellular ATP level in conditioned media of cultured cells, 1.0 x 10^6 MDCK cells, MDCK-pTR GFP-RasV12 cells, or MDCK-pTR GFP-caspase-8 cells were seeded on collagen-coated 35-mm dish (Greiner) and incubated for 12 h. Culture media were then changed to FBS-free DMEM containing tetracycline and the indicated inhibitor, followed by the measurement after 3 h (for MDCK-pTR GFP-caspase-8) or 16 h (for MDCK-pTR GFP-RasV12). For Scribble-knockdown cells, 4.0 x 10^5 MDCK-pTR Scribble-shRNA1 cells were seeded and treated as described above except that following 12 h incubation after seeding, cells were treated with tetracycline for 24 h, and culture media were changed to FBS-free DMEM containing tetracycline and the indicated inhibitor, followed by the measurement after 12 h. For the effect of Z-VAD-FMK, caspase-8-expressing cells were pretreated with Z-VAD-FMK for 2 h prior to tetracycline addition. Collected conditioned media were centrifuged at 111 x g for 5 min at 4°C, and 100 μL of supernatant were transferred into a white opaque 96-well plate (Thermo Fisher Scientific). After 100 μL of CellTiter-Glo 2.0 reagent (Promega) was added into the 96-well plate, the plate was horizontally shaken for 2 min and incubated for 10 min at room temperature. After the incubation, the luminescence was measured using Varioskan Flash (Thermo Fisher Scientific). The calibration of luminescence to ATP concentration was performed using ATP standard solutions of known concentration.

Mice

Villin-Cre^{ERT2} mice were crossed with CAG-loxP-STOP-loxP (LSL)-eGFP mice or DNMT1-CAG-LSL-$HRas^{V12}$-IRES-eGFP mice to generate villin-CreERT2-LSL-eGFP (villin-GFP) mice or -LSL-$HRas^{V12}$-IRES-eGFP (villin-RasV12-GFP) mice, respectively.[38] 6-12-week old C57BL/6 mice of either sex were used. For PCR genotyping of mice, primer sequences were as follow; Villin-CreERT2: 5'-CAAGCCTGGCTCGACGGCC-3' and 5'-CGCGAACATCTTCAGGTTCT-3', DNMT1-CAG-loxP-STOP-loxP-HRasV12-IRES-eGFP: 5'-CACTGTGGAATCTCGGCAGG-3' and 5'-GCAATATGGTGGAAAATAAC-3', and CAG-loxP-STOP-loxP-eGFP: 5'-CAGT-CAGTTGCTCAATGTACC-3' and 5'-ACTGGTGAAACTCACCCA-3'. Villin-RasV12-GFP or villin-GFP mice were given a single intraperitoneal injection of 1 or 0.5 mg of tamoxifen, respectively, in corn oil (Sigma) per 20 g of body weight, and mice were then sacrificed at 3 days after Cre activation. To examine the effect of Trolox on oxidative stress in intestinal epithelia, villin-RasV12-GFP mice were first administrated with 50 mg/kg of Trolox (Sigma-Aldrich) in corn oil by intraperitoneal injection at days 0 and 2. Subsequently, the mice were injected intraperitoneally with 1.0 mg of tamoxifen at day 3. After 24 h of tamoxifen injection, the mice were intraperitoneally administrated with 50 mg/kg of Trolox at days 4 and 5 and then sacrificed at day 6. To culture intestinal organoids, isolated crypts from the mouse small intestine were entrapped in matrigel (Corning) and plated in a non-coated 35-mm glass-bottom dish as previously described.[38] The crypts embedded in matrigel were covered with cultured media (Advanced DMEM/F12, Gibco) supplemented with N2 (Invitrogen), B27 (Invitrogen), 50 ng/mL EGF (PeproTech), 100 ng/mL Noggin (PeproTech), 1.25 mM N-acetylcysteine (NAC) (Sigma-Aldrich), and the R-spondin conditioned medium collected from 293T-HA-Rspol-Fc cells provided by Dr. Calvin Kuo (Stanford University). After 96 h culture, organoids were incubated in the culture media without B27 and NAC and treated with 100 nM tamoxifen (Sigma) for 24 h to induce transgenes. Subsequently, tamoxifen was washed out, and organoids were incubated with CellROX for 1 h or fixed with 4% PFA. To examine the effect of Trolox or Apyrase ex vivo, organoids were incubated in the culture medium without B27 and NAC and were treated with 100 nM tamoxifen in the absence or presence of Trolox or apyrase for 24 h.

QUANTIFICATION AND STATICAL ANALYSIS

Statistics analysis

To compare the difference between two groups, unpaired or paired two-tailed Student's t tests were conducted. For multiple comparisons, one-way ANOVA with Dunnett's test or Tukey's test was performed. Mann-Whitney test was conducted in Figures 6J and S6H. p values less than 0.05 were considered to be significant. No statistical method was used to predetermine sample size.

Current Biology, Volume *32*

Supplemental Information

Extracellular ATP facilitates cell extrusion from epithelial layers mediated by cell competition or apoptosis

Yusuke Mori, Naoka Shiratsuchi, Nanami Sato, Azusa Chaya, Nobuyuki Tanimura, Susumu Ishikawa, Mugihiko Kato, Ikumi Kameda, Shunsuke Kon, Yukinari Haraoka, Tohru Ishitani, and Yasuyuki Fujita

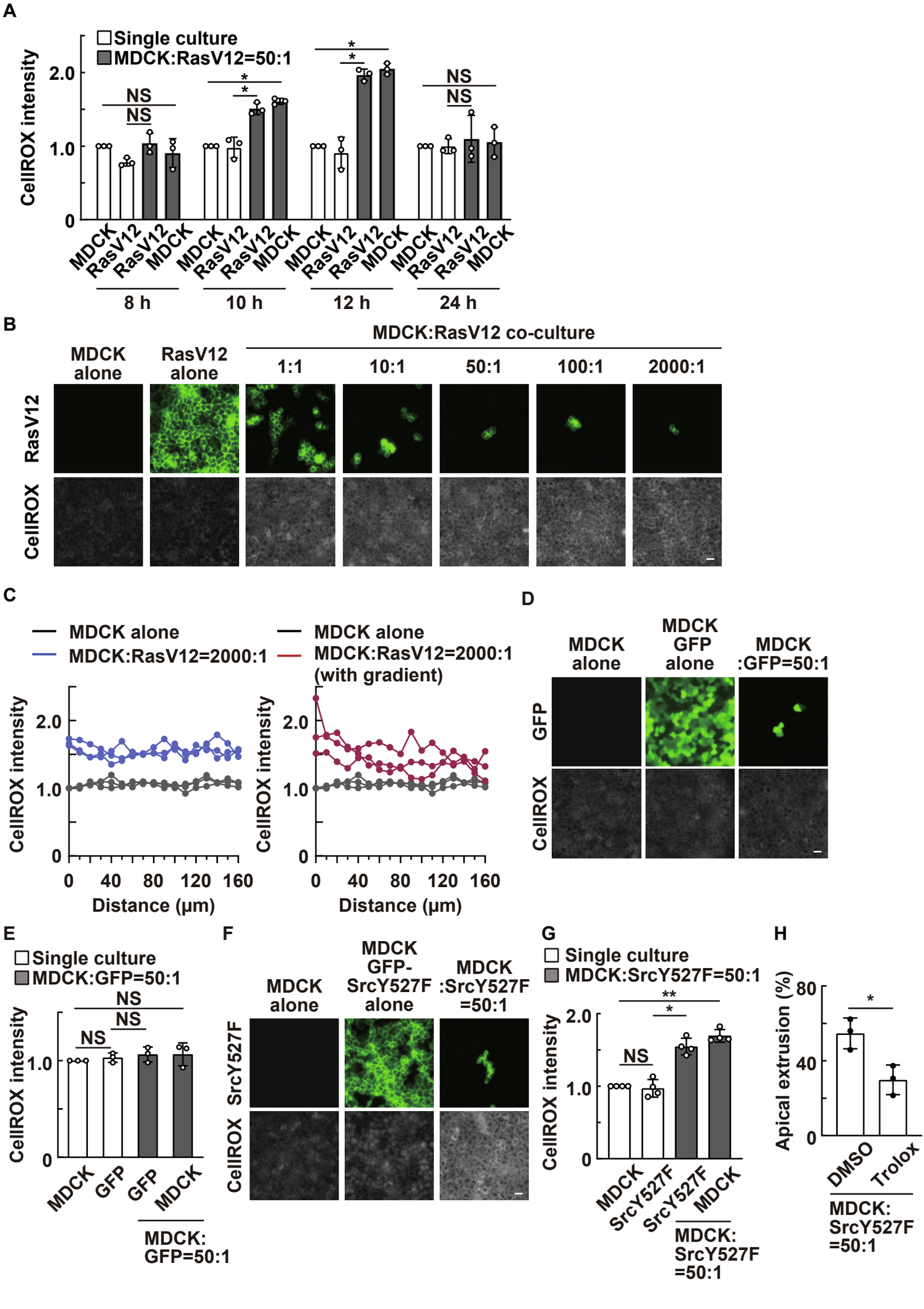
A
Single culture
MDCK:RasV12=50:1
CellROX intensity
2.0
1.0
0
NS
NS
*
*
*
*
NS
NS
MDCK
RasV12
RasV12
MDCK
8 h
10 h
12 h
24 h
B
MDCK:RasV12 co-culture
MDCK alone
RasV12 alone
1:1
10:1
50:1
100:1
2000:1
RasV12
CellROX
C
MDCK alone
MDCK:RasV12=2000:1
MDCK alone
MDCK:RasV12=2000:1 (with gradient)
CellROX intensity
2.0
1.0
0
0
40
80
120
160
Distance (μm)
D
MDCK alone
MDCK GFP alone
MDCK :GFP=50:1
GFP
CellROX
E
Single culture
MDCK:GFP=50:1
CellROX intensity
1.0
0
NS
NS
NS
MDCK
GFP
GFP
MDCK
MDCK: GFP=50:1
F
MDCK alone
MDCK GFP-SrcY527F alone
MDCK :SrcY527F =50:1
SrcY527F
CellROX
G
Single culture
MDCK:SrcY527F=50:1
CellROX intensity
2.0
1.0
0
**
*
NS
MDCK
SrcY527F
SrcY527F
MDCK
MDCK: SrcY527F =50:1
H
Apical extrusion (%)
80
40
0
*
DMSO
Trolox
MDCK: SrcY527F =50:1

Figure S1. ROS promote apical extrusion of SrcY527F-transformed cells from the epithelial layer, related to Figure 1

(A) The intracellular ROS level in the single- or co-cultured normal and RasV12-transformed cells. Normal MDCK cells and MDCK-pTR GFP-RasV12 cells were cultured alone or co-cultured at a ratio of 50:1, followed by the treatment with tetracycline for 8, 10, 12, or 24 h, and the intracellular ROS level was examined by CellROX. Values are expressed as a ratio relative to single-cultured MDCK cells at each time point. Data are mean ± SD from three independent experiments. *$p < 0.05$ and NS: not significant (paired two-tailed Student's t-test); n = 180, 180, 117, 293, 180, 180, 180, 310, 180, 180, 156, 352, 180, 180, 121, and 341 cells.

(B) Intracellular ROS level in the single- or co-cultured normal and RasV12-transformed cells at various mixing ratios. Normal MDCK cells and MDCK-pTR GFP-RasV12 cells were cultured alone or co-cultured at a ratio of 1:1, 10:1, 50:1, 100:1, or 2,000:1, followed by the treatment with tetracycline for 16 h, and the intracellular ROS level was examined by CellROX.

(C) Quantification of fluorescent intensity of CellROX in the surrounding normal cells within 160 μm from RasV12-transformed cells. MDCK cells were cultured alone or co-cultured with MDCK-pTR GFP-RasV12 cells at a ratio of 2,000:1, followed by CellROX analysis. For MDCK cells cultured alone, CellROX fluorescent intensity was measured within 160 μm from randomly selected cells. Values are expressed as a ratio relative to MDCK cells alone at 0 μm. Three representative results are shown for cells that show evenly distributed (left) or gradually decreased CellROX intensity around RasV12 cells (right).

(D and E) The intracellular ROS level in single- or co-cultured normal and GFP-expressing cells. Normal MDCK and MDCK-pTR GFP cells were cultured alone or co-cultured at a ratio of 50:1, followed by CellROX analysis. (D) CellROX fluorescent images. (E) Quantification of fluorescent intensity of CellROX. Values are expressed as a ratio relative to single-cultured MDCK cells. Data are mean ± SD from three independent experiments. NS: not significant (one-way ANOVA with Tukey's test); n = 166, 166, 162, and 126 cells.

(F and G) The intracellular ROS level in single- or co-cultured normal and SrcY527F-transformed cells. Normal MDCK cells and MDCK-pTR GFP-SrcY527F cells were cultured alone or co-cultured at a ratio of 50:1, followed by CellROX analysis. (F) CellROX fluorescent images. (G) Quantification of fluorescent intensity of CellROX. Values are expressed as a ratio relative to single-cultured MDCK cells. Data are mean ± SD from four independent experiments. *$p < 0.05$, ** $p< 0.01$, and NS: not significant (one-way ANOVA with Tukey's test); n = 240, 240, 130, and 360 cells.

(H) Effect of Trolox on apical extrusion of SrcY527F-transformed cells surrounded by normal cells. Data are mean ± SD from three independent experiments. *$p < 0.05$ (paired two-tailed Student’s t-test); n = 292 and 293 cells.

(B, D, and F) Scale bars, 20 μm.

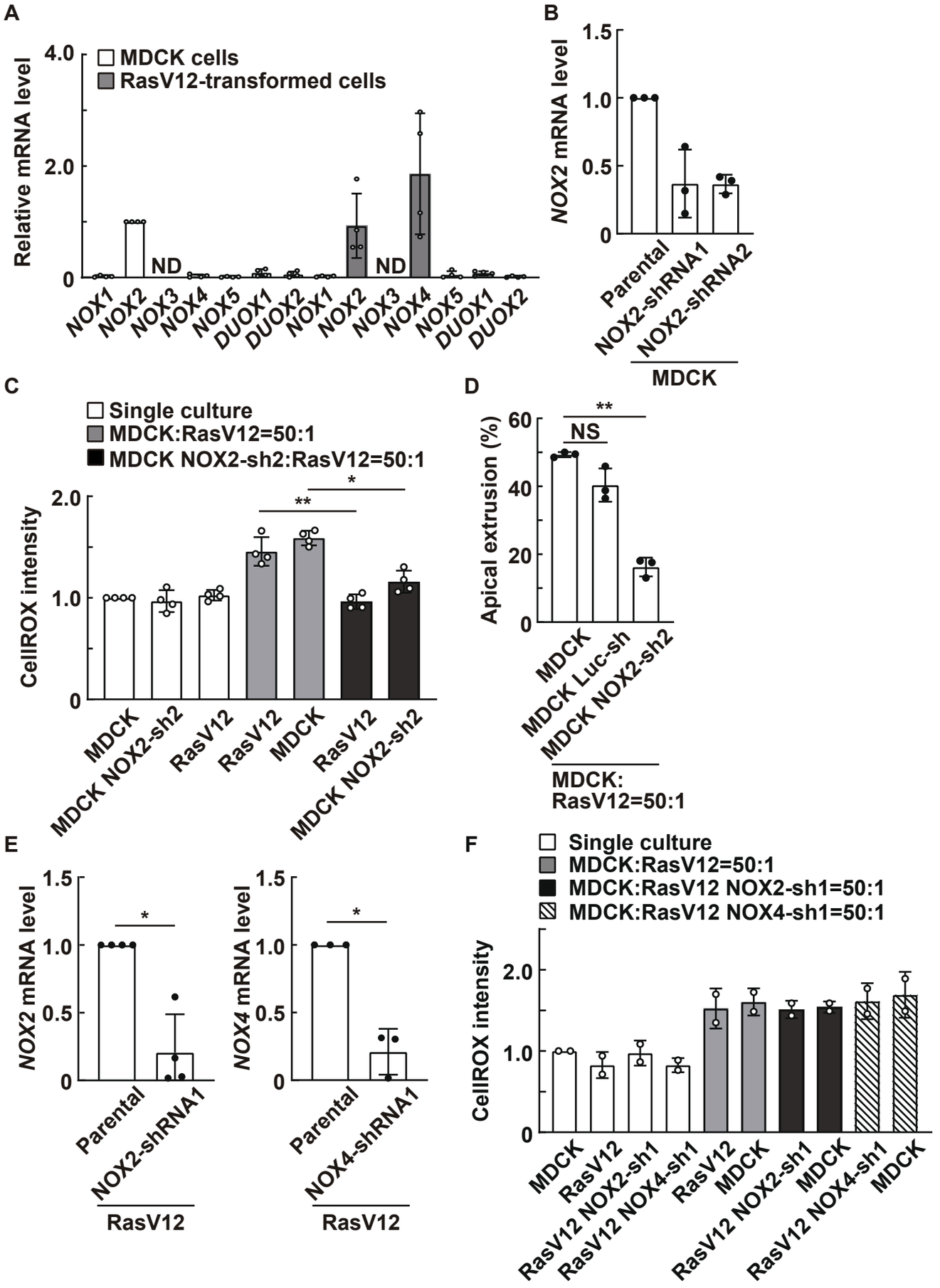
A
MDCK cells
RasV12-transformed cells
Relative mRNA level
4.0
2.0
0
ND
ND
NOX1
NOX2
NOX3
NOX4
NOX5
DUOX1
DUOX2
NOX1
NOX2
NOX3
NOX4
NOX5
DUOX1
DUOX2
B
NOX2 mRNA level
1.5
1.0
0.5
0
Parental
NOX2-shRNA1
NOX2-shRNA2
MDCK
C
Single culture
MDCK:RasV12=50:1
MDCK NOX2-sh2:RasV12=50:1
CellROX intensity
2.0
1.0
0
*
**
MDCK
MDCK NOX2-sh2
RasV12
RasV12
MDCK
RasV12
MDCK NOX2-sh2
D
**
NS
Apical extrusion (%)
60
40
20
0
MDCK
MDCK Luc-sh
MDCK NOX2-sh2
MDCK:
RasV12=50:1
E
NOX2 mRNA level
1.5
1.0
0.5
0
*
Parental
NOX2-shRNA1
RasV12
NOX4 mRNA level
1.5
1.0
0.5
0
*
Parental
NOX4-shRNA1
RasV12
F
Single culture
MDCK:RasV12=50:1
MDCK:RasV12 NOX2-sh1=50:1
MDCK:RasV12 NOX4-sh1=50:1
CellROX intensity
2.0
1.0
0
MDCK
RasV12
RasV12 NOX2-sh1
RasV12 NOX4-sh1
RasV12
MDCK
RasV12 NOX2-sh1
MDCK
RasV12 NOX4-sh1
MDCK

Figure S2. NOX2 in surrounding normal cells promotes apical extrusion of RasV12-transformed cells, related to Figure 2

(A) Quantitative real-time PCR analysis of NADPH oxidases in normal cells or RasV12-transformed cells cultured alone. Values are expressed as a ratio relative to *NOX2* expression in MDCK cells. Data are mean ± SD from four independent experiments. ND: not detected.

(B) Effect of NOX2-shRNA expression on the *NOX2* mRNA level in MDCK cells. Values are expressed as a ratio relative to parental MDCK cells. Data are mean ± SD from three independent experiments.

(C and D) Effect of NOX2-knockdown in surrounding cells on the intracellular ROS level (C) and apical extrusion (D). (C) Quantification of fluorescent intensity of CellROX. MDCK-pTR GFP-RasV12 cells were cultured alone or co-cultured with normal MDCK or MDCK NOX2-shRNA2 cells at a ratio of 1:50, followed by CellROX analysis. Values are expressed as a ratio relative to single-cultured MDCK cells. Data are mean ± SD from four independent experiments. *$p < 0.05$ and **$p < 0.01$ (one-way ANOVA with Dunnett's test); n = 240, 240, 240, 266, 638, 190, and 448 cells.

(D) Effect of NOX2-knockdown in surrounding cells on apical extrusion of RasV12-transformed cells. Data are mean ± SD from three independent experiments. **$p < 0.01$ and NS: not significant (one-way ANOVA with Dunnett's test); n = 362, 324, and 409 cells.

(E) Effect of NOX2-shRNA or NOX4-shRNA expression on the *NOX2* or *NOX4* mRNA level in MDCK-pTR GFP-RasV12 cells respectively. Data are mean ± SD from three (for NOX4) or four (for NOX2) independent experiments. *$p < 0.05$ (paired two-tailed Student's t-test).

(F) Effect of NOX2-knockdown or NOX4-knockdown in RasV12-transformed cells on the intracellular ROS level. MDCK-pTR GFP-RasV12, MDCK-pTR GFP-RasV12 NOX2-shRNA1, or MDCK-pTR GFP-RasV12 NOX4-shRNA1 cells were cultured alone or co-cultured with normal MDCK cells at a ratio of 1:50, followed by CellROX analysis. Values are expressed as a ratio relative to single-cultured MDCK cells. Data are mean ± SD from two independent experiments; n = 120, 120, 120, 120, 94, 262, 94, 199, 70, and 100 cells.

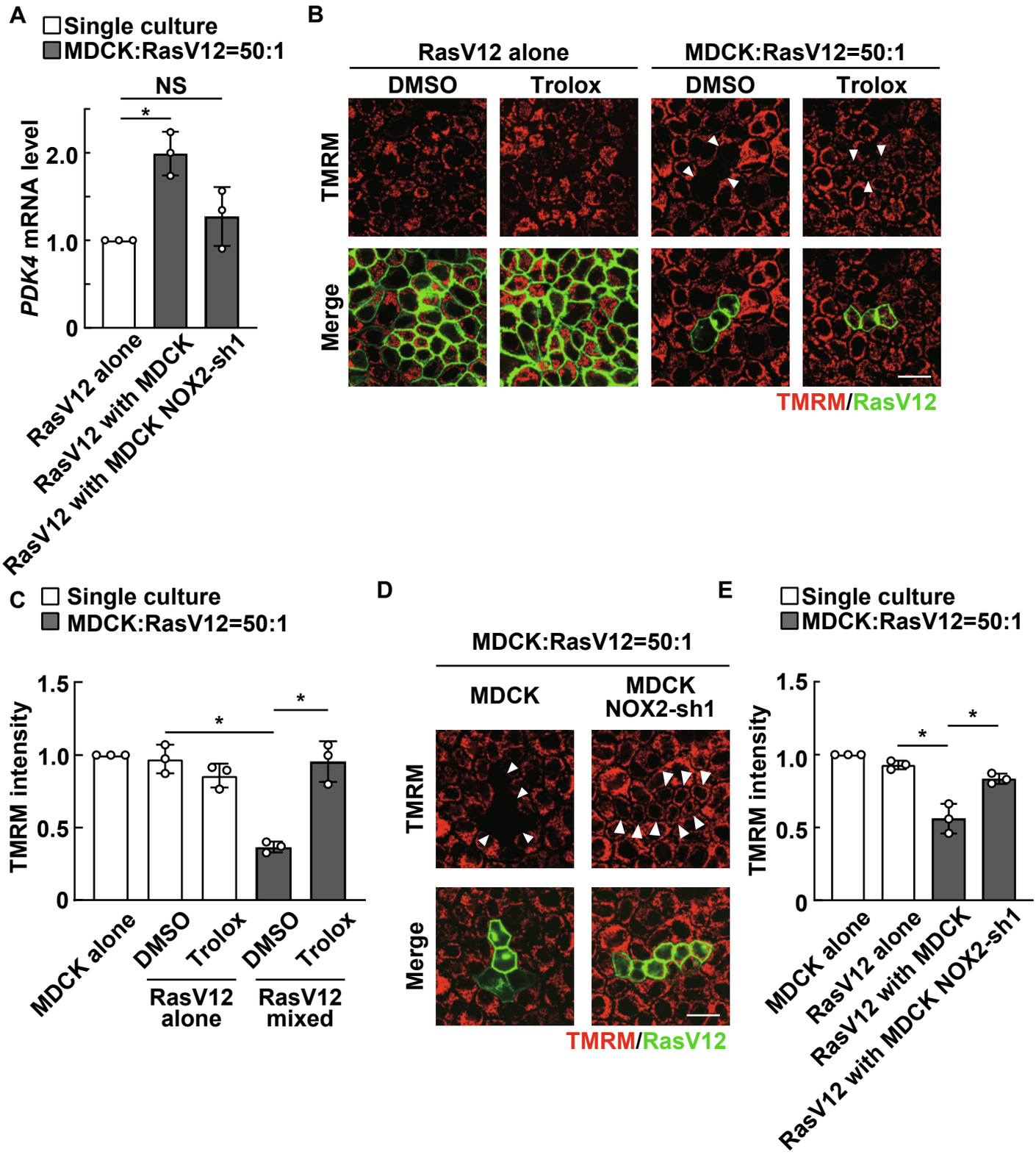
A
Single culture
MDCK:RasV12=50:1
NS
*
PDK4 mRNA level
2.0
1.0
0
RasV12 alone
RasV12 with MDCK
RasV12 with MDCK NOX2-sh1
B
RasV12 alone
MDCK:RasV12=50:1
DMSO
Trolox
DMSO
Trolox
TMRM
Merge
TMRM/RasV12
C
Single culture
MDCK:RasV12=50:1
TMRM intensity
1.5
1.0
0.5
0
*
*
MDCK alone
DMSO
Trolox
DMSO
Trolox
RasV12 alone
RasV12 mixed
D
MDCK:RasV12=50:1
MDCK
MDCK NOX2-sh1
TMRM
Merge
TMRM/RasV12
E
Single culture
MDCK:RasV12=50:1
TMRM intensity
1.5
1.0
0.5
0
*
*
MDCK alone
RasV12 alone
RasV12 with MDCK
RasV12 with MDCK NOX2-sh1

Figure S3. ROS induce the decreased mitochondrial membrane potential in RasV12-transformed cells surrounded by normal cells, related to Figure 2

(A) Effect of NOX2-knockdown in surrounding cells on the *PDK4* mRNA level in RasV12-transformed cells. MDCK-pTR GFP-RasV12 cells were cultured alone or co-cultured with normal MDCK or MDCK NOX2-shRNA cells at a ratio of 1:10. GFP-positive RasV12 cells were selectively collected by FACS sorting and subjected to qPCR analysis. Values are expressed as a ratio relative to RasV12 cells cultured alone. Data are mean ± SD from three independent experiments. *$p < 0.05$ and NS: not significant (one-way ANOVA with Dunnett's test).

(B and C) Effect of Trolox on the TMRM incorporation in RasV12-transformed cells surrounded by normal cells. MDCK-pTR GFP-RasV12 cells were cultured alone or co-cultured with normal MDCK cells at a ratio of 1:50 in the absence or presence of Trolox, followed by loading with TMRM. (B) TMRM fluorescent images. Arrowheads indicate RasV12 cells surrounded by normal cells. (C) Quantification of fluorescent intensity of TMRM. Values are expressed as a ratio relative to single-cultured MDCK cells. Data are mean ± SD from three independent experiments. *$p < 0.05$ (one-way ANOVA with Dunnett's test); n = 240, 240, 240, 285, and 210 cells.

(D and E) Effect of NOX2-knockdown in surrounding cells on the TMRM incorporation in RasV12-transformed cells. MDCK-pTR GFP-RasV12 cells were co-cultured with normal MDCK or MDCK NOX2-shRNA1 cells at a ratio of 1:50, followed by loading with TMRM. (D) TMRM fluorescent images. Arrowheads indicate RasV12 cells. (E) Quantification of fluorescent intensity of TMRM. Values are expressed as a ratio relative to single-cultured MDCK cells. Data are mean ± SD from

three independent experiments. *$p < 0.05$ (one-way ANOVA with Dunnett's test); n = 180, 180, 199, and 353 cells.

(B and D) Scale bars, 20 μm.

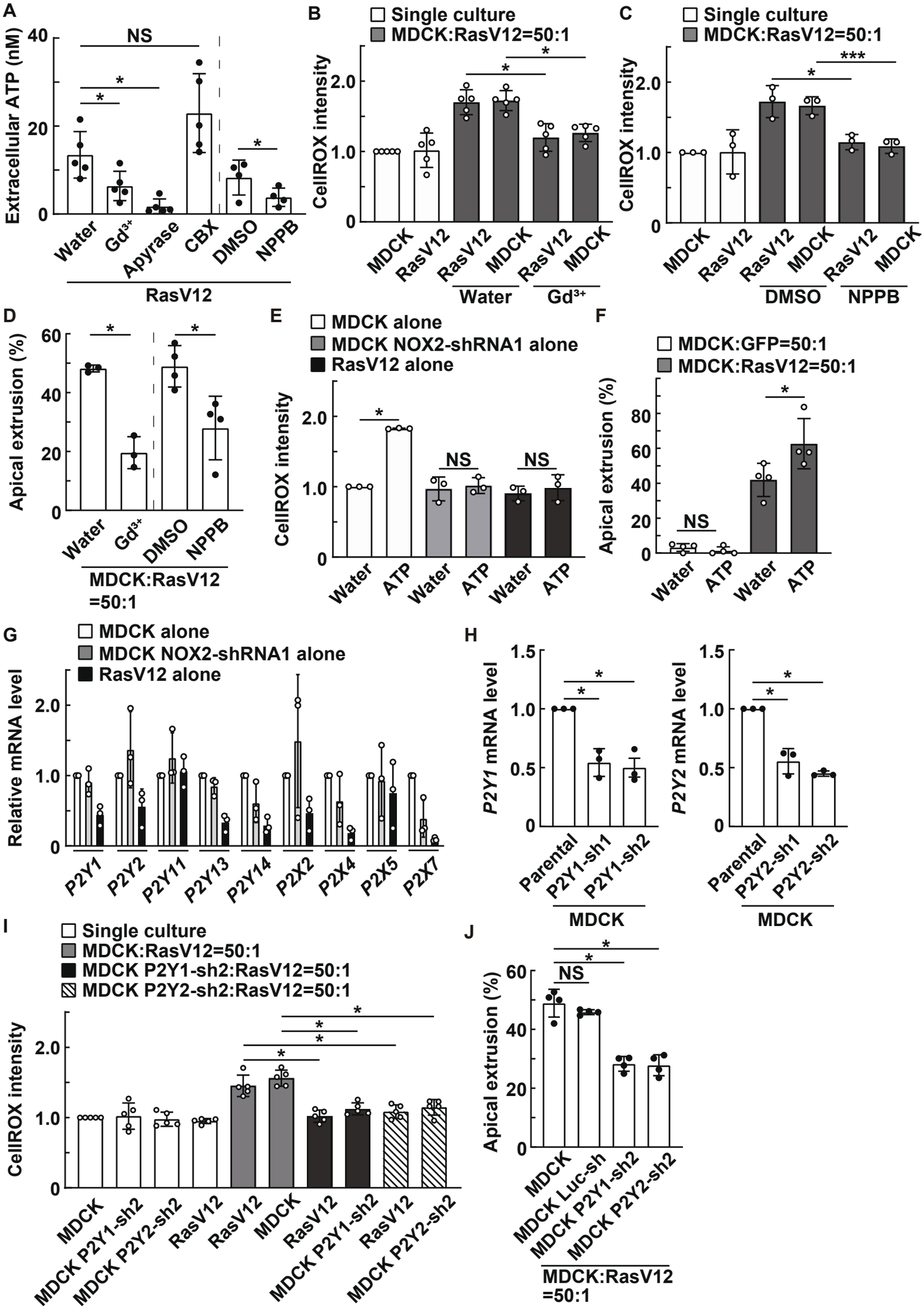
A
Extracellular ATP (nM)
NS
Water
Gd3+
Apyrase
CBX
DMSO
NPPB
RasV12
B
Single culture
MDCK:RasV12=50:1
CellROX intensity
MDCK
RasV12
Water
Gd3+
C
Single culture
MDCK:RasV12=50:1
CellROX intensity
DMSO
NPPB
D
Apical extrusion (%)
Water
Gd3+
DMSO
NPPB
MDCK:RasV12 =50:1
E
MDCK alone
MDCK NOX2-shRNA1 alone
RasV12 alone
CellROX intensity
NS
Water
ATP
F
MDCK:GFP=50:1
MDCK:RasV12=50:1
Apical extrusion (%)
NS
G
MDCK alone
MDCK NOX2-shRNA1 alone
RasV12 alone
Relative mRNA level
P2Y1
P2Y2
P2Y11
P2Y13
P2Y14
P2X2
P2X4
P2X5
P2X7
H
P2Y1 mRNA level
Parental
P2Y1-sh1
P2Y1-sh2
MDCK
P2Y2 mRNA level
P2Y2-sh1
P2Y2-sh2
I
Single culture
MDCK:RasV12=50:1
MDCK P2Y1-sh2:RasV12=50:1
MDCK P2Y2-sh2:RasV12=50:1
CellROX intensity
MDCK
MDCK P2Y1-sh2
MDCK P2Y2-sh2
RasV12
MDCK P2Y1-sh2
MDCK P2Y2-sh2
J
Apical extrusion (%)
NS
MDCK
MDCK Luc-sh
MDCK P2Y1-sh2
MDCK P2Y2-sh2
MDCK:RasV12 =50:1

Figure S4. Extracellular ATP signal via P2Y1 or P2Y2 receptor in surrounding cells promotes apical extrusion of RasV12-transformed cells, related to Figure 3

(A) Effect of an inhibitor for ATP release channel on the extracellular ATP level of RasV12-transformed cells. MDCK-pTR GFP-Rasv12 cells were treated with Gd^{3+}, apyrase, CBX, or NPPB, and the extracellular ATP level in conditioned media was measured using CellTiter-Glo 2.0 reagent. Data are mean ± SD from four (right two) or five (left four) independent experiments. *p<0.05 and NS: not significant (paired two-tailed Student's t-test (right two) or one-way ANOVA with Dunnett's test (left four)).

(B-D) Effect of Gd^{3+} or NPPB treatment on the intracellular ROS level (B and C) or apical extrusion (D). (B and C) Quantification of fluorescent intensity of CellROX. Normal MDCK and MDCK-pTR GFP-RasV12 cells were cultured alone or co-cultured in the absence or presence of Gd^{3+} (B) or NPPB (C), followed by CellROX analysis. Values are expressed as a ratio relative to single-cultured MDCK cells. Data are mean ± SD from five (B) or three (C) independent experiments. *p < 0.05 and ***p < 0.001 (one-way ANOVA with Dunnett's test); n = 299, 300, 266, 657, 217, and 473 cells (B) or 179, 185, 139, 312, 86, and 274 cells (C). (D) Effect of Gd^{3+} or NPPB treatment on apical extrusion of RasV12-transformed cells. Data are mean ± SD from three (Water- or Gd^{3+}-treated cells) or four (DMSO- or NPPB-treated cells) independent experiments. *p < 0.05 (paired two-tailed Student's t-test); n = 355, 400, 499, and 346 cells.

(E and F) Effect of exogenous ATP treatment on the intracellular ROS level (E) or apical extrusion (F). (E) Quantification of fluorescent intensity of CellROX. Normal MDCK, MDCK NOX2-shRNA1, or MDCK-pTR GFP-RasV12 cells were cultured alone in the absence or presence of exogenous ATP for 30 min, followed by CellROX analysis. Values are expressed as a ratio relative to water-treated MDCK cells. Data are

mean ± SD from three independent experiments. *p < 0.05 and NS: not significant (paired two-tailed Student's t-test); n = 180 cells for all conditions. (F) Quantification of apical extrusion of RasV12 cells. MDCK-pTR GFP or MDCK-pTR GFP-RasV12 cells were co-cultured with normal MDCK cells at a ratio of 1:50 in the absence or presence of exogenous ATP for 24 h. Data are mean ± SD from four independent experiments. *p < 0.05 and NS: not significant (paired two-tailed Student's t-test); n = 358, 402, 400, and 356 cells.

(G) Quantitative real-time PCR analysis of the P2Y or P2X receptors in normal MDCK, MDCK NOX2-shRNA1, or MDCK-pTR GFP-RasV12 cells. Values are expressed as a ratio relative to MDCK cells. Data are mean ± SD from three independent experiments. Note that the expression of *P2Y4*, *P2Y6*, *P2Y12*, *P2X1*, *P2X3*, or *P2X6* was not detected in this qPCR analysis.

(H) Effect of P2Y1-shRNA or P2Y2-shRNA expression on the *P2Y1* or *P2Y2* mRNA level in MDCK cells. Data are mean ± SD from three independent experiments. *p < 0.05 (one-way ANOVA with Dunnett's test).

(I and J) Effect of P2Y1- or P2Y2-knockdown in surrounding cells on the intracellular ROS level (I) or apical extrusion (J). (I) Quantification of fluorescent intensity of CellROX. MDCK-pTR GFP-RasV12 cells were cultured alone or co-cultured with normal MDCK, MDCK P2Y1-shRNA2, or MDCK P2Y2-shRNA2 cells, followed by CellROX analysis. Values are expressed as a ratio relative to single-cultured MDCK cells. Data are mean ± SD from five independent experiments. *p < 0.05 (one-way ANOVA with Dunnett's test); n = 300, 300, 300, 300, 217, 427, 234, 460, 180, and 325 cells. (J) Effect of P2Y1- or P2Y2-knockdown in surrounding cells on apical extrusion of RasV12-transformed cells. Data are mean ± SD from four independent experiments.

*$p < 0.05$ and NS: not significant (one-way ANOVA with Dunnett's test); n = 424, 525, 528, and 550 cells.

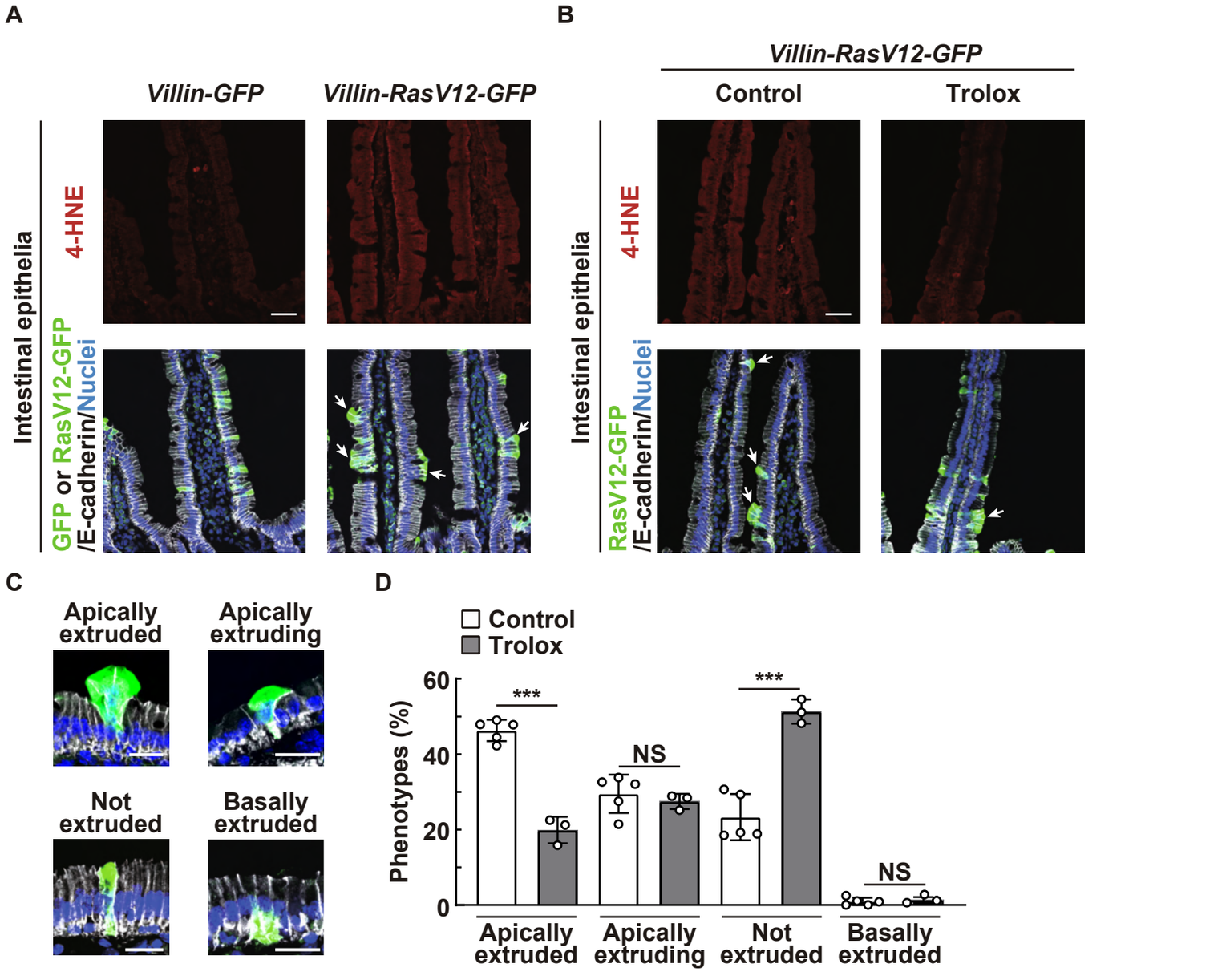
A
Villin-GFP
Villin-RasV12-GFP
Intestinal epithelia
4-HNE
GFP or RasV12-GFP
/E-cadherin/Nuclei
B
Villin-RasV12-GFP
Control
Trolox
Intestinal epithelia
4-HNE
RasV12-GFP
/E-cadherin/Nuclei
C
Apically extruded
Apically extruding
Not extruded
Basally extruded
D
Control
Trolox
Phenotypes (%)
60
40
20
0
***
NS
***
NS
Apically extruded
Apically extruding
Not extruded
Basally extruded

Figure S5. Oxidative stress promotes apical extrusion of RasV12-transformed cells from mouse intestinal epithelia, related to Figure 4

(A and B) Immunofluorescent analysis for 4-HNE in intestinal epithelia from *villin-Cre^{ERT2}-LSL-eGFP* or *-LSL-Ras^{V12}-IRES-eGFP* mice at 3 days after tamoxifen administration with or without Trolox treatment. The arrows indicate apically extruded or extruding RasV12-expressing cells.

(C) Classification of the phenotypes of RasV12-expressing cells in intestinal epithelia of *villin-Cre^{ERT2}-LSL-Ras^{V12}-IRES-eGFP* mice. 'apically extruded': completely detached from the basement membrane and translocated into the apical lumen. 'apically extruding': with their nucleus apically shifted, but still attached to the basement membrane. 'not extruded': remaining within the epithelium. 'Basally extruded': basally delaminated from the epithelial layer.

(D) Quantification of the phenotypes of RasV12-expressing cells in intestinal epithelia at 3 days after tamoxifen administration with or without Trolox treatment. Data are mean ± SD from three independent experiments. ***$p < 0.001$ and NS: not significant (unpaired two-tailed Student's t-test); n = 1,258 or 855 cells from five (Control) or three (Trolox) mice, respectively.

Scale bars, 40 μm (A and B) or 20 μm (C).

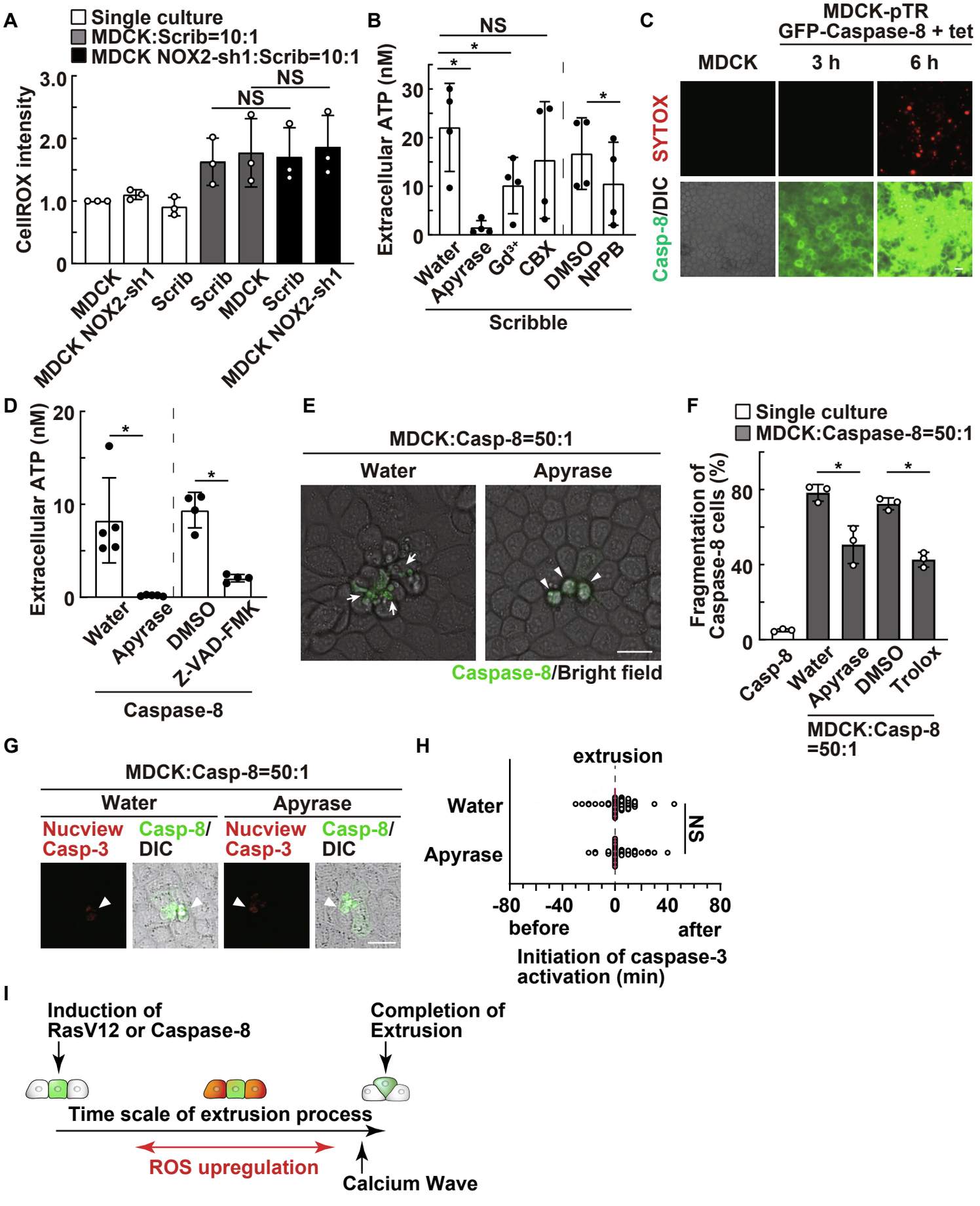
A
Single culture
MDCK:Scrib=10:1
MDCK NOX2-sh1:Scrib=10:1
CellROX intensity
3.0
2.0
1.0
0
NS
NS
MDCK
MDCK NOX2-sh1
Scrib
Scrib
MDCK
Scrib
MDCK NOX2-sh1
B
NS
*
*
Extracellular ATP (nM)
30
20
10
0
*
Water
Apyrase
Gd3+
CBX
DMSO
NPPB
Scribble
C
MDCK-pTR
GFP-Caspase-8 + tet
MDCK
3 h
6 h
SYTOX
Casp-8/DIC
D
Extracellular ATP (nM)
20
10
0
*
*
Water
Apyrase
DMSO
Z-VAD-FMK
Caspase-8
E
MDCK:Casp-8=50:1
Water
Apyrase
Caspase-8/Bright field
F
Single culture
MDCK:Caspase-8=50:1
Fragmentation of Caspase-8 cells (%)
80
40
0
*
*
Casp-8
Water
Apyrase
DMSO
Trolox
MDCK:Casp-8 =50:1
G
MDCK:Casp-8=50:1
Water
Apyrase
Nucview Casp-3
Casp-8/ DIC
Nucview Casp-3
Casp-8/ DIC
H
extrusion
Water
Apyrase
SN
-80
-40
0
40
80
before
after
Initiation of caspase-3 activation (min)
I
Induction of RasV12 or Caspase-8
Completion of Extrusion
Time scale of extrusion process
ROS upregulation
Calcium Wave

Figure S6. Extracellular ATP and ROS pathways affect the behavior and fate of caspase-8-expressing cells surrounded by normal cells, related to Figures 5 and 6

(A) Effect of NOX2-knockdown in surrounding cells on the intracellular ROS level. MDCK-pTR Scribble-shRNA1 cells were cultured alone or co-cultured with normal MDCK or MDCK NOX2-shRNA1 cells at a ratio of 1:10, followed by CellROX analysis. Values are expressed as a ratio relative to single-cultured MDCK cells. Data are mean ± SD from three independent experiments. NS: not significant (one-way ANOVA with Dunnett's test); n = 180, 175, 180, 208, 400, 194, and 364 cells.

(B) Effect of an inhibitor for ATP release channel on the extracellular ATP level of Scribble-knockdown cells. MDCK-pTR Scribble-shRNA1 cells were treated with apyrase, Gd^{3+}, CBX, or NPPB, and the extracellular ATP level in conditioned media was measured using CellTiter-Glo 2.0 reagent. Data are mean ± SD from four independent experiments. *$p < 0.05$ and NS: not significant (one-way ANOVA with Dunnett's test (left four) or paired two-tailed Student's t-test (right two)).

(C) Effect of caspase-8 expression on the membrane integrity. Normal MDCK cells or MDCK-pTR GFP-caspase-8 cells were cultured alone, followed by the treatment with tetracycline for 3 or 6 h. Cells were then stained with SYTOX-dye to analyze the membrane integrity.

(D) Effect of apyrase or Z-VAD-FMK on the extracellular ATP level of caspase-8-expressing cells. MDCK-pTR GFP-caspase-8 cells were treated with apyrase or Z-VAD-FMK, and the extracellular ATP level in conditioned media was measured using CellTiter-Glo 2.0 reagent. Data are mean ± SD from five (Water- or apyrase-treated) or four (DMSO- or Z-VAD-FMK-treated) independent experiments. *$p < 0.05$ (paired two-tailed Student's t-test).

(E and F) Effect of apyrase or Trolox on the fragmentation of caspase-8-expressing cells within an epithelial monolayer. (E) Representative images of caspase-8-expressing cells treated with apyrase. MDCK-pTR GFP-caspase-8 cells were co-cultured with normal MDCK cells in the absence or presence of apyrase. Images were extracted from a representative time-lapse analysis (Videos S1 and S2). The arrows or arrowheads indicate fragmented or intact caspase-8-expressing cells, respectively. (F) Quantification of the fragmentation of caspase-8-expressing cells surrounded by normal cells in the absence or presence of apyrase or Trolox. Data are mean ± SD from three independent experiments. *$p < 0.05$ (paired two-tailed Student's t-test); n = 94, 177, 158, 130, and 170 cells.

(G and H) Effect of apyrase on caspase-3 activation in caspase-8-expressing cells surrounded by normal cells. (G) Representative images for the caspase-3 activity indicator Nucview. Normal MDCK and MDCK-pTR GFP-caspase-8 cells were co-cultured at a ratio of 50:1 in the absence or presence of apyrase, followed by the time-lapse observation. The activity of caspase-3 was monitored using Nucview. Arrowheads indicate caspase-8-expressing cells upon extrusion just prior to fragmentation. (H) The timing of initiation of caspase-3 activation in caspase-8-expressing cells extruded with the fragmentation phenotype in the absence or presence of apyrase. Red bars indicate median values. NS: not significant (Mann-Whitney test); n= 85 and 45 cells from three independent experiments.

(I) A schematic of the time scale of the extrusion process of RasV12-transformed or caspase-8-expressing cells from the epithelial layer.

(C, E, and G) Scale bars, 20 μm.

Inhibitors	Targets	ROS level	Apical extrusion
α-GA	gap junction	No effect	↓*
GsMTX	mechanosensitive calcium channel	No effect	↓*
Ibuprofen	cyclooxygenase	No effect	↑*
Trolox	ROS	↓*	↓*
Y27632	Rho kinase	No effect	↓*
Blebbistatin	Myosin-II	No effect	↓*
BAY117082	NF-κB	No effect	ND
VAS2870	NADPH oxidase	↓*	↓*
CCCP	mitochondrial oxidative phosphorylation	No effect	ND
Nocotazole	microtubule	No effect	↓*
CK666	Arp2/3 complex	No effect	↓*
SMIFTH2	formin	No effect	↓*
ML141	Cdc42	No effect	ND
H89	PKA	No effect	ND
U0126	MEK	No effect	↓*
LY294002	PI3K	No effect	↓*
Apyrase	extracellular ATP	↓*	↓*
Suramin	P2Y, P2X receptor	↓*	↓*
$AgNO_3$	Aquaporin	No effect	ND
GW4869	exosome biogenesis/ release	No effect	ND

Table S1. Effects of various inhibitors on the ROS level and apical extrusion, related to Figures 1-3

Normal MDCK cells were co-cultured with MDCK-pTR GFP-RasV12 cells at a ratio of 50:1 in the presence of the indicated inhibitor. *Statistically significant (paired two-tailed Student's t-test or one-way ANOVA with Dunnet's test); ND: not done; gray box: the indicated data are based on our published observations.

Oligonucleotides	**Sequence**
NOX2-shRNA1 forward	GATCCCCCTGGTTCTATGGGGTTTATTTCAAGAGAATAAACCCCATAGAACCAGTTTTTC
NOX2-shRNA1 reverse	TCGAGAAAAACTGGTTCTATGGGGTTTAT TCTCTTGAAATAAACCCCATAGAACCAGGGG
NOX2-shRNA2 forward	GATCCCCCACCAGAATAGGAGTTTTTTTCAAGAGAAAAAACTCCTATTCTGGTGTTTTTC
NOX2-shRNA2 reverse	TCGAGAAAAACACCAGAATAGGAGTTTTTTCTCTTGAAAAAAACTCCTATTCTGGTGGGG
NOX4-shRNA1 forward	GATCCCCTAGGAAAAACTAATATTTATTCAAGAGATAAATATTAGTTTTTCCTATTTTTC
NOX4-shRNA1 reverse	TCGAGAAAAATAGGAAAAACTAATATTTATCTCTTGAATAAATATTAGTTTTTCCTAGGG
P2Y1-shRNA1 forward	GATCCCCCACGTTACATCCATTGTTTTTCAAGAGAAAACAATGGATGTAACGTGTTTTTC
P2Y1-shRNA1 reverse	TCGAGAAAAACACGTTACATCCATTGTTTTCTCTTGAAAAACAATGGATGTAACGTGGGG
P2Y1-shRNA2 forward	GATCCCCCGCTCATCTTCTACTACTTTTCAAGAGAAAGTAGTAGAAGATGAGCGTTTTTC
P2Y1-shRNA2 reverse	TCGAGAAAAACGCTCATCTTCTACTACTT TCTCTTGAAAAGTAGTAGAAGATGAGCGGGG
P2Y2-shRNA1 forward	GATCCCCGCCAATGAATGGGCAACTTTTCAAGAGAAAGTTGCCCATTCATTGGCTTTTTC
P2Y2-shRNA1 reverse	TCGAGAAAAAGCCAATGAATGGGCAACTTTCTCTTGAAAAGTTGCCCATTCATTGGCGGG
P2Y2-shRNA2 forward	GATCCCCGGCTACAAGTGCCGTTTCATTCAAGAGATGAAACGGCACTTGTAGCCTTTTTC
P2Y2-shRNA2 reverse	TCGAGAAAAAGGCTACAAGTGCCGTTTCATCTCTTGAATGAAACGGCACTTGTAGCCGGG
Luciferase-shRNA forward	GATCCCCTGAAACGATATGGGCTGAATTCAAGAGATTCAGCCCATATCGTTTCATTTTTC
Luciferase-shRNA reverse	TCGAGAAAAATGAAACGATATGGGCTGAATCTCTTGAATTCAGCCCATATCGTTTCAGGG
Primer, NOX1 forward	CTGGGTAGTTAACCACTGGTTCTC
Primer, NOX1 reverse	GCTTTCTCATATGACAGGAAGGC
Primer, NOX2 forward	GCAATAACGCCACTAACCTGAG
Primer, NOX2 reverse	AGCAAGTCCGCAAACCACTC
Primer, NOX3 forward	CTCAAATTCCACAAACTGGTCG
Primer, NOX3 reverse	TGACTGGCTCCAGTGGTAACG
Primer, NOX4 forward	GAAACTTCTGTTTGATGAAATAGC
Primer, NOX4 reverse	GTGAAGAGTCTTAGAAATTGAATTGG
Primer, NOX5 forward	GCGACTACTTGTACCTGAACATCC
Primer, NOX5 reverse	CATCTGGCTACACATCCGGTC

Primer, DUOX1 forward	TGACCCACCACCTCTACATCC
Primer, DUOX1 reverse	GATTAGTGCCGGGACCAGG
Primer, DUOX2 forward	ACGGCTTCCTCTCCAAGGAT
Primer, DUOX2 reverse	CCTTGTCCTGGAAGCCTGAC
Primer, PDK4 forward	CCTTTGGCTGGTTTTGGTTA
Primer, PDK4 reverse	TTGCCAGATTCTTTGGTTCC
Primer, P2Y1 forward	TGCTCATCCTGGGCTGCTAC
Primer, P2Y1 reverse	GGGATGTAGGACACGGCGAA
Primer, P2Y2 forward	AGTGCCGTTTCAATGAGGAC
Primer, P2Y2 reverse	TGCTGCAGTAAAGGTTGGTG
Primer, P2Y11 forward	TGAGTTCCTGGTGGCTGTGG
Primer, P2Y11 reverse	AGCAGCGTCAGGGCATAGAG
Primer, P2Y13 forward	CTTGGTGGCCGACCTGGTAA
Primer, P2Y13 reverse	AGCCGAGAAACGACACACGA
Primer, P2Y14 forward	AATCCCCTACACGCAGAGCC
Primer, P2Y14 reverse	GCATACGTTTGCAGCCGACA
Primer, P2X2 forward	AAGGACGGCTACCTGAAACA
Primer, P2X2 reverse	GTCCAGGTCACAGTCCCAGT
Primer, P2X4 forward	GCAACAGGAAAATGCGTGCT
Primer, P2X4 reverse	AGAGTGAAGTTTTCTGCAGCCT
Primer, P2X5 forward	GAACAAGAAGGTGGGCCTGC
Primer, P2X5 reverse	CTGCAGGGAGGTGTCAGTGT
Primer, P2X7 forward	CCTGCTGCAGCTGTAACGAT
Primer, P2X7 reverse	GTTGGTACCGCTTGTCACTGA
Primer, β-actin forward	GGCACCCAGCACAATGAAG
Primer, β-actin reverse	ACAGTGAGGCCAGGATGGAG

Table S2. Oligonucleotides used in this study. Related to STAR Methods.